K-L-6195-2

A DESIGN MODEL FOR THE DYNAMIC ADSORPTION OF URANIUM HEXAFLUORIDE ON FIXED BEDS OF SODIUM FLUORIDE

UNION CARBIDE CORPORATION
NUCLEAR DIVISION
OAK RIDGE GASEOUS DIFFUSION PLANT

operated for the ATOMIC ENERGY COMMISSION *under* U. S. GOVERNMENT Contract W-7405 eng 26

UNION CARBIDE

OAK RIDGE GASEOUS DIFFUSION PLANT
P. O. Box P
Oak Ridge, Tennessee 37830

DISCLAIMER

Report Number: K-L-6195-2

A DESIGN MODEL FOR THE DYNAMIC ADSORPTION OF URANIUM HEXAFLUORIDE ON FIXED BEDS OF SODIUM FLUORIDE

A Thesis

Presented to

the Graduate Council of

The University of Tennessee

In Partial Fulfillment

of the Requirements for the Degree

Master of Science

by

Michael J. Stephenson

December 1968

ACKNOWLEDGEMENTS

The author wishes to express his appreciation to his major advisor, Dr. D. I. Dunthorn, of the Gaseous Diffusion Development Division of the Oak Ridge Gaseous Diffusion Plant (operated by Union Carbide Corporation for the U. S. Atomic Energy Commission) and the Chemical Engineering Department of the University of Tennessee. Dr. Dunthorn's valuable suggestions, encouragement, and unlimited patience were instrumental to the success of this project.

The writer is also indebted to several other members of the Gaseous Diffusion Development Division, particularly to Mr. J. H. Pashley, Mr. L. W. Anderson, and Mr. J. R. Merriman, whose support made this work possible, and to Dr. J. L. Snyder for his helpful comments and final review of the project.

The author wishes to thank Mrs. Georgia Anderson of the Gaseous Diffusion Development Division for her excellent typing and the help received in the preparation of this manuscript.

Finally, the author expresses his deepest appreciation to his wife, Ellen, for her understanding and often needed encouragement, and to his parents, Mr. and Mrs. A. F. Stephenson, for their continued effort and concern.

ABSTRACT

A mathematical model has been developed that describes the dynamic adsorption of uranium hexafluoride on fixed beds of sodium fluoride. This model is intended for the design engineer as a means of sizing sodium fluoride traps for use in uranium hexafluoride collection and purification. The analysis, which requires a digital computer program, is limited to isothermal, isobaric systems where the concentration of uranium hexafluoride in the feed gas is less than ten mole percent.

Data obtained from reported experiments with the uranium hexafluoride-sodium fluoride system are compared with calculated results, the closeness of agreement establishing the reliability of the model within the range covered by available data. A discussion of general results is given, including the dependence of adsorber performance upon pellet properties and other physical parameters as implied by the behavior of the model.

TABLE OF CONTENTS

CHAPTER		PAGE
I.	INTRODUCTION	1
II.	LITERATURE REVIEW	2
	Mass Transfer Correlations	5
	Diffusion Within a Porous Structure	7
	Point Rate of Reaction of Uranium Hexafluoride on Sodium Fluoride	10
	Bulk Effects of Uranium Hexafluoride Adsorption on Diffusion	11
III.	THEORY	12
	Adsorption in a Fixed Bed	12
	Simultaneous Diffusion and First-Order Reaction in a Porous Solid	13
	Simplification of the Equations Pertaining to Fixed-Bed Adsorption	14
	Solution of the Simplified Equations	16
IV.	DETERMINATION OF EMPIRICAL CONSTANTS FROM EXPERIMENTAL DIFFERENTIAL BED DATA	19
	Experimental Differential Bed Data	20
	Results of Constant Determination	21
V.	COMPARISON OF RESULTS WITH EXPERIMENTAL FIXED-BED STUDIES	33
	Fixed-Bed Breakthrough Data	33

CHAPTER PAGE

Results of the Comparison 35

VI. DISCUSSION OF RESULTS 42

Effects of Total Gas Flow and Concentration 43

Effect of Temperature 45

Effect of Pellet Surface Area 45

Adsorber Operation 49

Determination of the Maximum Pellet Loading 50

VII. CONCLUSIONS AND RECOMMENDATIONS 51

Conclusions 51

Recommendations 51

LIST OF REFERENCES 53

APPENDIXES 57

A. FORTRAN PROGRAM FOR SOLUTION OF THE MODEL EQUATIONS 58

B. DIFFUSION COEFFICIENTS IN BINARY GAS SYSTEMS 65

C. VISCOSITY OF BINARY GAS MIXTURES 67

D. ACCURACY OF THE NUMERICAL SOLUTION 69

E. ESTIMATION OF MAXIMUM PELLET LOADING 72

LIST OF SYMBOLS 75

VITA 78

LIST OF FIGURES

FIGURE PAGE

1. Comparison of Computed with Experimental Differential Bed Loading at 84°F and 2.62 Mole Percent Uranium Hexafluoride 22
2. Comparison of Computed with Experimental Differential Bed Loading at 122°F and 2.35 Mole Percent Uranium Hexafluoride 23
3. Comparison of Computed with Experimental Differential Bed Loading at 199°F and 1.69 Mole Percent Uranium Hexafluoride 24
4. Comparison of Computed with Experimental Differential Bed Loading at 212°F and 0.57 Mole Percent Uranium Hexafluoride 25
5. Comparison of Computed with Experimental Differential Bed Loading at 212°F and 2.45 Mole Percent Uranium Hexafluoride 26
6. Comparison of Computed with Experimental Differential Bed Loading at 212°F, 1.69 Mole Percent Uranium Hexafluoride, and 0.428 Pellet Void Fraction 27
7. Comparison of Computed with Experimental Differential Bed Loading at 212°F, 1.69 Mole Percent Uranium Hexafluoride, and 0.386 Pellet Void Fraction 28

FIGURE PAGE

8. Comparison of Computed with Experimental Differential Bed Loading at 302°F and 1.69 Mole Percent Uranium Hexafluoride 29

9. Relationship of Reaction Rate Constant C_2 with Maximum Pellet Loading 31

10. Comparison of Predicted Breakthrough Curves with Experimental Data at 200°F and Total Gas Flow Rate of 7.01 lb mole/sq ft-hr 36

11. Comparison of Predicted Breakthrough Curves with Experimental Data at 200°F and Total Gas Flow Rate of 5.57 lb mole/sq ft-hr 37

12. Comparison of Predicted Breakthrough Curves with Experimental Data at 225°F 38

13. Comparison of Predicted Breakthrough Curves with Experimental Data at 250°F 39

14. Comparison of Predicted Breakthrough Curves with Experimental Data at 250°F, Using High Surface Area Pellets 40

15. Required Pellet Bed Depth as a Function of Total Gas Flow Rate and Uranium Concentration at 250°F 44

16. Required Pellet Bed Depth as a Function of Total Gas Flow Rate and Uranium Concentration at 200°F 46

17. Required Pellet Bed Depth as a Function of Pellet Surface Area and On-Stream Time 47

FIGURE PAGE

18. Convergence Behavior of Numerical Solution for Typical Run 70

19. Predicted Maximum Pellet Loading as a Function of Temperature and Pellet Surface Area 73

20. Predicted Maximum Pellet Loading as a Function of Temperature and Pellet Void Fraction 74

CHAPTER I

INTRODUCTION

Increasing demand for enriched uranium for power and research reactors has placed a heavy burden upon the uranium industry. The U. S. Atomic Energy Commission is sponsoring many development programs designed to expand existing uranium technology, aiding private industry in preparing itself to achieve predicted production heights. The problem areas considered by the Atomic Energy Commission are diverse and range from uranium enrichment to reprocessing of spent reactor fuels.

Methods of collection and purification of the uranium product, usually in the form of volatile uranium hexafluoride, are of wide interest to the industry. Current nuclear reactor designs require enriched uranium, necessitating preparation of uranium hexafluoride to allow concentration of the U-235 isotope. Specifications for the uranium hexafluoride supplied to the AEC limit concentrations for most impurities to the parts per million range [2].

Cold traps are frequently used for the large-scale collection of gaseous uranium hexafluoride by desublimation from a noncondensing carrier gas [10]. In search of a method for removing volatile fission products and other impurities from uranium hexafluoride and because of the difficulty in removing small concentrations (1 mole percent or less) of uranium hexafluoride from the process off-gas by cold trapping, attention has also been given to adsorption processes for the purification

and collection of uranium. Gaseous uranium hexafluoride was found to react with sodium fluoride, forming a solid complex, and because of the reversible nature of the reaction, sodium fluoride was investigated as a solid sorbent for separating uranium hexafluoride from other volatile species and condensing gases and as an alternative to low temperature cold trapping for collecting uranium hexafluoride. Sodium fluoride proved to be a very effective solid sorbent for both proposed applications.

The uranium hexafluoride-sodium fluoride reaction has been observed by a number of workers [6,15,16,17,22], but because of the difficult nature of the reaction kinetics, limited work is reported that actually attempts to formulate a rate equation characteristic of the process [17]. Consequently, the accepted guidelines from which sodium fluoride traps have been sized evolved primarily from prior operational experience, and the mathematical model of an adsorption system presented here, which describes the removal of gaseous uranium hexafluoride by pelletized sodium fluoride, should be quite valuable in future design work. The adsorption problem under consideration is relatively complex, involving a mechanism that employs variable reaction and diffusion rates, and does not lend itself to hand calculation. Therefore, the mathematical model for the adsorption system has been developed as a design tool by using a high-speed digital computer to perform the calculations.

CHAPTER II

LITERATURE REVIEW

When a gas is brought into equilibrium with a solid or liquid surface, the gas molecules tend to adsorb, or concentrate, in the immediate vicinity of the surface due to the attractive forces that exist between the two phases, regardless of the particular gas or surface considered. The strength of the attractive force varies widely, depending upon the particular system involved, from the relatively weak van der Waals force to a much stronger interaction of a chemical nature. The surface interaction referred to as adsorption is to be distinguished from absorption, which is the bulk diffusion of the gas specie into the structure of the solid or liquid. The term "sorption" is commonly used to describe the case where both adsorption and absorption may be occurring simultaneously.

The weaker van der Waals forces, associated with capillary condensation and liquefaction, are responsible for the particular adsorption mechanism labeled physical adsorption. At the other extreme, much stronger forces, relating to actual chemical bonding between atoms or molecules of the contacting phases, characterize activated adsorption or chemisorption processes. Several characterizations of adsorption phenomena are available [14,28] to differentiate clearly between the two types of adsorption processes. The heats of physical adsorption are of the same order of magnitude as heats of liquefaction of the respective adsorbing gases, whereas the heats of chemisorption are often in the

neighborhood of heats of chemical reaction. Physical adsorption processes are typically controlled by resistance to mass transfer, are more pronounced at low temperatures and high partial pressures, and decrease sharply as the partial pressure of the adsorbing component is decreased. On the other hand, chemisorption processes are usually controlled by resistance to surface reaction, and exhibit adsorption rates which characteristically increase with an increase in temperature, typical of chemical reactions involving an energy of activation. Physical adsorption is essentially nonspecific and, like condensation, will generally occur with any gas-solid system with the proper combination of temperature and pressure. Chemisorption, in contrast, will take place only if there is actual chemical bonding between the adsorbing gas and the surface atoms of the adsorbent.

The adsorption of uranium hexafluoride by sodium fluoride pellets is of the activated type, forming complexes with the reported formulae $UF_6 \cdot 3\ NaF$ [6], $UF_6 \cdot 2NaF$ [15], and $UF_6 \cdot NaF$ [16]. Katz [15] reports the dissociation pressure of the $UF_6 \cdot 2NaF$ complex to be

$$\text{Log}_{10} P_{mm} = 9.25 \pm 0.02 - (4.18 \cdot 10^3)/T_k, \qquad (1)$$

where p_{mm} = dissociation pressure, mm Hg, and

T_k = temperature, °K.

A heat of dissociation of - 19.1 ± 0.2 kilocalories per mole of evolved gas is given, calculated from the experimental data.

The adsorption of a molecule from a gas mixture by a solid porous pellet can be, in general, described by a three-step mechanism: diffusion of the molecule from the bulk gas stream to the external surface of the pellet, diffusion of the molecule into the pores of the pellet, and adsorption of the molecule on the pore surface. As discussed by McNeese [17], when uranium hexafluoride is adsorbed on sodium fluoride, an additional step must be considered to account for the diffusion of uranium hexafluoride from the internal surface of the pellet through a layer of complex to unreacted sodium fluoride.

Mass Transfer Correlations

Considerable work has been reported in the field of heat and mass transfer in flow of fluids through fixed beds of spherical particles. Gamson [12], in 1951, developed a correlation for a mass transfer factor for fluids in a fixed bed of spherical particles using a modified Reynolds number defined as

$$N_{Re'} \equiv \frac{D_p G}{\mu(1 - \varepsilon_B)}, \tag{2}$$

where D_p = effective particle diameter, ft,

G = mass flow rate of gas mixture, lb/hr-sq ft,

μ = viscosity of gas mixture, lb/ft-hr, and

ε_B = porosity of sorbent bed, dimensionless.

Gamson reported that

$$j_d = 17(N_{Re'})^{-1} (1 - \varepsilon_B)^{0.2} \tag{3}$$

for $N_{Re'}$ less than about 10, and that

$$j_d = 1.46\ (N_{Re'})^{-0.41}\ (1 - \varepsilon_B)^{0.2} \qquad (4)$$

for $N_{Re'}$ greater than 100. The "j" factor for mass transfer is defined as

$$j_d \equiv \frac{K_g\ P_{gf}}{(G/M_m)}\ \left(\frac{\mu}{\rho D_{AB}}\right)^{2/3},$$

where K_g = overall mass transfer coefficient, lb-mole/hr-sq ft-atm,

P_{gf} = log-mean partial pressure of inert component in "film", atm,

G = mass flow rate of gas mixture, lb/hr-sq ft,

M_m = average molecular weight of gas mixture, lb/lb-mole,

μ = viscosity of gas mixture, lb/ft-hr,

ρ = density of gas mixture, lb/cu ft, and

D_{AB} = diffusivity of component A in B, sq ft/hr.

Gamson did not attempt to obtain an expression for j_d between modified Reynolds numbers of 10 and 100 as an apparent transition existed in this region.

Bradshaw and Myers [5], using the same modified Reynolds number as Gamson, attempted to correlate mass transfer data for spheres and cylinders in a fixed bed with a least squares fit using an equation of the form

$$j_d = a\ (N_{Re'})^b. \qquad (5)$$

The final equation, reported as

$$j_d = 2.25\ (N_{Re'})^{-0.501}, \qquad (6)$$

yielded a good correlation of available data for higher flows, i.e., $N_{Re'} > 400$, but was not extended to lower Reynolds numbers.

Gupta and Thodos [13], in 1962, contended that there appeared to be no real justification for modifying the Reynolds number by the introduction of a factor containing the void fraction. In view of this, Gupta and Thodos attempted to correlate transfer factors with the conventional Reynolds number. The relationship representing the data best was expressed by the equation

$$\varepsilon_B \, j_d = 0.010 + \frac{0.863}{N_{Re}^{0.58} - 0.483}. \qquad (7)$$

The equation was restricted to the region $N_{Re} > 1$ because of the lack of transfer data for lower flows.

Diffusion Within a Porous Structure

Mass transfer within a porous media has been the subject of much attention as the reactivity, selectivity, and other important characteristics of heterogeneous catalysis are dependent upon pore structure. The description of the diffusion phenomena occurring within the irregular set of passageways present in most porous solids is usually represented by a single effective diffusion coefficient, D_{eff}. The effective diffusion coefficient depends on the properties of the gases, on the temperature and pressure, and on the pore structure. Depending upon the pore size, two main types of diffusion must be considered: Knudsen (or molecular) diffusion, which occurs when the pore diameter is small compared to the mean free path of the diffusing species, and ordinary (or

bulk) diffusion, which occurs when the pore diameter is large when compared to the mean free path. Wheeler [27] recommends that the effective diffusion coefficient in pores of any size and at any gas pressure be represented by

$$D_{eff} = D_{AB} \left[1 - e^{-(D_K/D_{AB})}\right]. \tag{8}$$

The Knudsen diffusion contribution, D_K, is given by Wheeler as

$$D_K = 9.7 \cdot 10^3 \, r_p \sqrt{T/M}, \tag{9}$$

where D_K = Knudsen diffusion coefficient, sq cm/sec,

r_p = pore radius, cm,

T = temperature, °K, and

M = molecular weight, g/g-mole,

and the bulk diffusion coefficient of the gas specie A in B, D_{AB}, at the temperature and pressure system, is given as

$$D_{AB} = D^{\circ}_{AB} \left(\frac{T}{273}\right)^{1.75} \frac{1}{P}, \tag{10}$$

where D°_{AB} is the diffusion coefficient at 1 atmosphere and 0°C.

Wakao and Smith [24,25] proposed a theory for predicting diffusion rates with and without reaction at constant pressure through bi-disperse porous media, considering diffusion through macro- and micropores. A knowledge of the pore volume-pore radius distribution for the porous material is required to apply the theory. For low density pellets, however, only the macropore contribution should be significant. If the Knudsen part of the diffusion in the macropores is negligible, as is the case if the macropores are large enough or the pressure high enough, the

theory predicts a simple relationship of the form

$$D_{eff} = \varepsilon^2 D_{AB} \cdot \tag{11}$$

Satterfield and Sherwood [21] use

$$D_{AB,eff} = D_{AB} \varepsilon/\tau \tag{12}$$

for ordinary, or bulk, diffusion in a porous solid and

$$D_{K,eff} = D_K \varepsilon/\tau \tag{13}$$

for Knudsen diffusion, where τ is termed the "tortuosity" factor, allowing for both tortuosity and varying pore cross section within the solid. For estimation of D_{eff} in the transition region between ordinary and Knudsen diffusion, Satterfield and Sherwood propose

$$\frac{1}{D_{eff}} = \frac{1}{D_{K,eff}} + \frac{1}{D_{AB,eff}} \tag{14}$$

as an approximation. For solids having bimodal pore size distribution, τ has been found to range between 0.37 and 0.83.

Bulk diffusion is inversely proportional to pressure. Since Knudsen diffusion is independent of pressure, the diffusion of gases in porous materials is dependent on the total pressure only as the overall diffusion rate is dependent on the bulk diffusion mechanism. The effect of temperature depends on the relative importance of both mechanisms, since the temperature influence on each mechanism is significant and different.

Point Rate of Reaction of Uranium Hexafluoride on Sodium Fluoride

McNeese [17] formulated an expression for the point rate of reaction of uranium hexafluoride with sodium fluoride:

$$\frac{dq_r}{dt} = C_1 \rho_{NaF} S \, e^{-(E/RT)} \, e^{-(C_2 q_r / \rho_{NaF} S)} \, C, \qquad (15)$$

where q_r = amount of uranium hexafluoride complexed at a given radius, r, within the pellet, lb/cu ft,

t = time, hr,

C_1 = empirical constant, cu ft/lb-hr-(area/mass),

ρ_{NaF} = density of sodium fluoride pellet, lb/cu ft,

S = surface area of sodium fluoride pellet, area/mass,

E = activation energy for diffusion, Btu/lb mole,

R = gas constant, Btu/lb mole-°R,

T = temperature, °R,

C_2 = empirical constant, area/mass, and

C = concentration of gaseous uranium hexafluoride within the pellet at the point of reaction, lb UF_6/cu ft.

By defining a pseudo-first-order rate reaction constant,

$$k_1' \equiv C_1 \rho_{NaF} S \, e^{-(E/RT)} \, e^{-(C_2 q_r / \rho_{NaF} S)}, \qquad (16)$$

the rate equation becomes

$$\frac{dq_r}{dt} = k_1' C \quad . \qquad (17)$$

Bulk Effects of Uranium Hexafluoride Adsorption on Diffusion

As implied by Equation (15), the point reaction rate is a function of the amount of uranium hexafluoride complex and is therefore a function of position within the pellet and varies with time as additional complex forms. Likewise, it is important to recognize that as complex is formed the void volume available for diffusion within the pellet decreases [17]. That is to say, the porosity, ε, of the pellet also changes with time and position within the pellet, and since the effective diffusion rate depends upon the pellet porosity, it, too, varies. Letting ε_o be the initial void fraction, an effective point porosity, ε_r, can be defined as

$$\varepsilon_r \equiv \varepsilon_o(1 - q_r/q_{max}) \ , \tag{18}$$

where q_{max} is the maximum quantity of uranium hexafluoride than can be reacted at any given point within the pellet. Consequently, the effective bulk diffusion coefficient assumes the form

$$D_{AB,eff} = D_{AB}\ \varepsilon_o(1 - q_r/q_{max})/\tau \ . \tag{19}$$

CHAPTER III

THEORY

The formulation of differential equations describing the removal of uranium hexafluoride from bulk gas with a fixed bed of sodium fluoride pellets is relatively straightforward. The solution of the equations, however, presents formidable problems unless certain simplifying assumptions are made. The validity of the assumptions must, of course, be ultimately tested by a comparison of predicted results against actual experimental results. The primary problems arise from the dependence of the local, or point, reaction and effective diffusion rates on the amounts of uranium hexafluoride already complexed within the pellet. The governing partial differential equations and the method of solution are presented in detail in this chapter.

Adsorption in a Fixed Bed

For the general case where adsorption takes place in a fixed-bed adsorber [14], under the assumptions of plug flow, negligible radial concentration gradients, negligible axial mixing, and constant temperature, a differential material balance on component A is

$$- G_N \left(\frac{\partial C_{Ab}}{\partial z}\right)_t = \rho_B \left(\frac{\partial q_A}{\partial t}\right)_z + \rho_G \varepsilon_B \left(\frac{\partial C_{Ab}}{\partial t}\right)_z , \qquad (20)$$

where G_N = mass flow rate of inert component, lb/hr-sq ft,

C_{Ab} = concentration of component A in bulk gas stream, lb of A/lb of inert component,

z = distance in bed, ft,

ρ_B = bulk density of adsorbent, lb/cu ft,

q_A = quantity of component A which has reacted, lb of A/lb of sorbent,

t = time, hr,

ρ_G = density of inert gas, lb/cu ft, and

ε_B = porosity of sorbent bed, dimensionless.

Simultaneous Diffusion and First-Order Reaction in a Porous Solid

Incorporating the concept of an effective or "average" diffusivity, the basic rate equation describing simultaneous diffusion and first-order reaction in a porous solid can be derived. Specifically, consider a spherical pellet of radius R submerged in a gas stream containing the adsorbing component A, the concentration of A being C_{As} on the external surface of the solid. Further, consider a spherical shell of thickness Δr contained within the pellet. The rate of diffusion of component A into the shell is

$$\text{Input} = 4\pi(r + \Delta r)^2 \left(D_{eff} + \frac{\partial D_{eff}}{\partial r} \Delta r\right) \frac{\partial}{\partial r} \left(C_A + \frac{\partial C_A}{\partial r} \Delta r\right), \qquad (21)$$

the rate of diffusion out of the shell is

$$\text{Output} = 4\pi r^2 D_{eff} \frac{\partial C_A}{\partial r}, \qquad (22)$$

the rate of reaction of component A within the shell is

$$\text{Reaction Rate} = 4\pi r^2 \, \Delta r \left(k_1' + \frac{1}{2} \frac{\partial k_1'}{\partial r} \Delta r\right)\left(C_A + \frac{1}{2} \frac{\partial C_A}{\partial r} \Delta r\right), \qquad (23)$$

and the rate of accumulation of component A in the pores of the pellet is

$$\text{Accumulation Rate} = 4\pi r^2 \, \Delta r \, \frac{\partial}{\partial t} \left[\left(\varepsilon + \frac{1}{2} \frac{\partial \varepsilon}{\partial r} \Delta r\right)\left(C_A + \frac{1}{2} \frac{\partial C_A}{\partial r} \Delta r\right)\right]. \qquad (24)$$

The pseudo rate constant k_1', effective diffusivity D_{eff}, and pellet porosity, ε, are considered as functions of radial position. Assumptions of radial symmetry, negligible temperature gradient, and homogeneity of physical and chemical pellet properties are implicit in the formulations of the rate equations.

Equating rate terms in a material balance, expanding, and letting Δr approach zero gives the partial differential equation:

$$\frac{\partial}{\partial t} (\varepsilon C_A) = D_{eff} \left[\frac{\partial^2 C_A}{\partial r^2} + \left(\frac{2}{r} + \frac{1}{D_{eff}} \frac{\partial D_{eff}}{\partial r}\right) \frac{\partial C_A}{\partial r}\right] - k_1' \, C_A. \qquad (25)$$

Simplification of the Equations Pertaining to Fixed-Bed Adsorption

As proposed by Hougen and Watson [14], for a steady-flow process, the last term of Equation (20) can be omitted if it is assumed that the fluid holdup of the bed is negligible. In this case,

$$- G_N \left(\frac{\partial C_{Ab}}{\partial z}\right)_t = \rho_B \left(\frac{\partial q_A}{\partial t}\right)_z . \qquad (26)$$

Crank [7] and Astarita [3] demonstrate that, for most reacting gas-solid systems, the accumulation of the adsorbing component in the pores

of the pellet is negligible compared to the other terms of the equation. Under this assumption, the basic differential equation describing the adsorption process within the pellet defines a quasi-steady-state profile given by

$$\frac{d^2C_A}{dr^2} + \left(\frac{2}{r} + \frac{1}{D_{eff}}\frac{dD_{eff}}{dr}\right)\frac{dC_A}{dr} - \frac{k_1'}{D_{eff}} C_A = 0. \qquad (27)$$

A finite-difference solution to Equation (27) was carried out by McNeese [17] but is too involved for practical application to fixed-bed adsorber calculations where finite-difference integration in both time and distance is also required; computation time requirements would be prohibitive for design studies. McNeese's solution does, however, provide an excellent means of predicting the maximum quantity of uranium hexafluoride that can be adsorbed by a specific sodium fluoride pellet in a given physical situation. The importance of the maximum loading at a point, q_{max}, has been shown in its influence on $D_{AB,eff}$, in Equation (19), and as will be demonstrated, the maximum loading capacity of the entire pellet plays an equally important role in correlation of experimental data.

Equation (27) may be further simplified by defining average quantities $\overline{k}_1$ and $\overline{D}_{eff}$ that are dependent upon the total pellet loading q and are, thereby, independent of radial position within the pellet. Thus, defining

$$\overline{k_1'} \equiv \overline{C}_1 \rho_{NaF} S \, e^{-(\overline{E}/RT)} \, e^{-(\overline{C}_2 \, q/S)} \qquad (28)$$

and

$$\bar{D}_{AB,eff} \equiv D_{AB}\, \varepsilon_o (1 - q/\bar{q}_{max})/\tau, \tag{29}$$

where $\bar{C}_1$, $\bar{E}$, $\bar{C}_2$, and $\bar{q}_{max}$ are representative quantities for the entire pellet. Equation (27) becomes the ordinary differential equation

$$\frac{d^2C_A}{dr^2} + \frac{2}{r}\frac{dC_A}{dr} = \frac{\bar{k}_1'}{\bar{D}_{eff}} C_A, \tag{30}$$

which further reduces to the more familiar form,

$$\bar{D}_{eff}\, \frac{1}{r^2}\frac{d}{dr}\left(r^2 \frac{dC_A}{dr}\right) = \bar{k}_1'\, C_A. \tag{31}$$

Solution of the Simplified Equations

With the boundary conditions that $C_A = C_{As}$ at $r = R$ and that C_A is finite at $r = 0$, the solution of Equation (31) is widely used [4,21,27] to describe diffusion and chemical reaction inside a porous catalyst and is given as

$$\frac{C_A}{C_{As}} = \frac{R}{r}\,\frac{\text{Sinh}\,(r\sqrt{\bar{k}_1'/\bar{D}_{eff}})}{\text{Sinh}\,(R\sqrt{\bar{k}_1'/\bar{D}_{eff}})}. \tag{32}$$

The mass flow of component A, W_{As}, per pellet at the surface $r = R$ is given by

$$W_{As} = \left[-4\pi R^2 \bar{D}_{eff} \frac{dC_A}{dr}\right]_{r=R} \tag{33}$$

or

$$W_{As} = 4\pi R D_{eff}\, C_{As}\left[R\sqrt{\bar{k}_1'/\bar{D}_{eff}}\ \text{Coth}\ (R\sqrt{\bar{k}_1'/\bar{D}_{eff}}) - 1\right] \tag{34}$$

where W_{As} = mass flow of component A at the surface of the pellet from bulk gas stream, lb/hr-pellet,

R = radius of spherical pellet, ft,

D_{eff} = average effective diffusivity of component A in B, sq ft/hr,

C_{As} = surface concentration of component A, lb/cu ft, and

k_1' = average pseudo-first-order reaction rate constant, 1/hr.

As presented by Bird, et al [4], for nonspherical particles, the foregoing results may be applied approximately by reinterpreting R. For nonspherical particles,

$$R_{nonsph} = 3 \left(\frac{V_p}{S_p}\right), \tag{35}$$

where V_p and S_p are the volume and external surface of a single pellet.

The use of Equation (34) requires knowledge of the surface concentration C_{As} of the reacting specie. By combining Equation (34) with the general equation for mass transfer across a stagnant gas film, incorporating an overall mass transfer coefficient predicted from one of the available correlations discussed earlier, the rate of removal of component A from the bulk gas stream by a single porous pellet can be determined. The equation for transfer across a stagnant gas film, using pressure equivalent driving force, is commonly given as [11]

$$N_{As} = K_g (P_{Ab} - P_{As}), \tag{36}$$

where N_{As} = molar flux of component A at the surface of the pellet, lb-mole/hr-sq ft,

K_g = overall mass transfer coefficient, lb-mole/hr-sq ft-atm,

P_{Ab} = partial pressure of component A in bulk gas stream, atm, and

P_{As} = partial pressure of component A on the exterior surface of the pellet, atm.

The mass flow of component A to the pellet from the bulk gas stream is

$$W_{As} = K_g \, a \, M_A \, (P_{Ab} - P_{As}), \tag{37}$$

where W_{As} = mass flow of component A at the surface of the pellet from the bulk gas, lb/hr-pellet.

a = effective mass transfer area, sq ft, and

M_A = molecular weight of component A, lb/lb-mole.

The total rate of reaction of component A with the pellet can be expressed as

$$r_A = \left(\frac{\partial q_A}{\partial t}\right)_z = \frac{W_{As}}{w} \tag{38}$$

where r_A = total rate of reaction of A with pellet, lb of A/lb of sorbent-hr, and

w = average weight of sorbent pellet, lb.

Equation (38), at any time t, establishes the total rate of reaction of component A at the differential bed segment z feet from the top of the sorbent bed, based upon the current pellet loading. By knowing the rate of reaction at a point z within the bed, a numerical integration [18] of Equation (26) can be performed to determine the concentration of component A leaving the differential bed segment at time t.

CHAPTER IV

DETERMINATION OF EMPIRICAL CONSTANTS FROM EXPERIMENTAL DIFFERENTIAL BED DATA

The reaction rate and diffusion equations for the uranium hexafluoride-sodium fluoride system were presented in Chapter II, and the necessary equations and their proposed simplified solutions describing the adsorption of uranium hexafluoride on fixed beds of pelleted sodium fluoride have been developed in Chapter III. In that presentation, several empirical or semi-empirical parameters were introduced. Specifically, these quantities are the reaction rate constants $\overline{C}_1$, $\overline{C}_2$, and $\overline{E}$ from Equation (28), tortuosity factor τ from Equation (29), and effective mass transfer area from Equation (37). In order to evaluate the empirical quantities, a computer program was written to perform all calculations necessary for the solution of the model equations. The entire program, written in FORTRAN IV, is listed in Appendix A. The program, as given, was run on both the IBM 7090 and IBM 360 computer systems. The results from the IBM 360 using single precision arithmetic agreed very well with those from the 7090, thus generally permitting calculations to be performed on the faster computer system operating in the faster mode. An abbreviated version of the FORTRAN IV program was recoded in FORTRAN II for use on a time-sharing SDS 940 computing system. This remote-access computer proved to be an invaluable tool in the critical analysis and understanding of the mathematical model and vastly

reduced the time required to arrive at values for the empirical constants.

Determination of the empirical constants involved a "brute force" approach, where values were manually adjusted until the mathematical model provided a best fit to several sets of data. The final results are displayed graphically to justify, at least to the accuracy required for design, the simplifying assumptions used in arriving at the model.

Experimental Differential Bed Data

Two sources of experimental data involving the uranium hexafluoride-sodium fluoride system were used in this investigation: the differential bed data of McNeese [17,25] and the fixed-bed breakthrough data of Anderson [1]. Because of the convenience in analyzing, the pellet loading data of McNeese were used for the determination of empirical constants. The data of Anderson are presented in Chapter V, in a final evaluation of the mathematical model.

McNeese determined the loading of uranium hexafluoride on single layers of sodium fluoride pellets during given time intervals, under different sets of operating conditions. For each run, a layer of sodium fluoride pellets was placed between two sections of glass beads contained within a 1-1/2-inch-diameter sorbent trap. A uranium hexafluoride-nitrogen gas mixture of known concentration and flow rate was then passed through the trap, which was maintained at a given temperature. After several runs of different durations, but under the same operating conditions and using pellets with the same physical properties, McNeese obtained a curve representing the loading of uranium hexafluoride on pelleted sodium fluoride as a function of time. Loading values,

expressed as the weight of uranium hexafluoride per unit weight of sodium fluoride, were obtained by actual weight difference before and after each run. Data were taken at atmospheric pressure over a temperature range of 84 to 302°F, and a uranium hexafluoride concentration range of 0.57 to 10.9 mole percent. The sodium fluoride pellets used in the tests were in the standard form of compacted right circular cylinders supplied by the Harshaw Chemical Company. The pellets had a surface area range of 0.69 to 1.05 sq m/g, a void fraction of 0.375 to 0.45, and had average weights of 0.0349 to 0.0398 g. The mean pore size varied from 4,600 to 6,800 A.

Results of Constant Determination

Eight different sets of differential bed loading data were used in the evaluation of the empirical constants, each data set being treated separately. Adjustments were made on the basis of individual comparisons, and new pellet loading curves were calculated until satisfactory fits were generated for all of the data sets. Final comparisons of pellet loading curves predicted by the model with the corresponding experimental data set are presented graphically in Figures 1 through 8. The expression for the pseudo reaction rate constant for the uranium hexafluoride-sodium fluoride system was determined to be

$$\bar{k}_1' = 32.6 \cdot 10^4 \rho_{NaF} S e^{-3816/T} e^{-\bar{C}_2 q/S} . \quad (39)$$

It was found to be most consistent and convenient to express C_2 as a function of maximum pellet loading and initial pellet porosity:

$$\bar{C}_2 = 3.147/[\bar{q}_{max} (1 - \varepsilon_o)]. \quad (40)$$

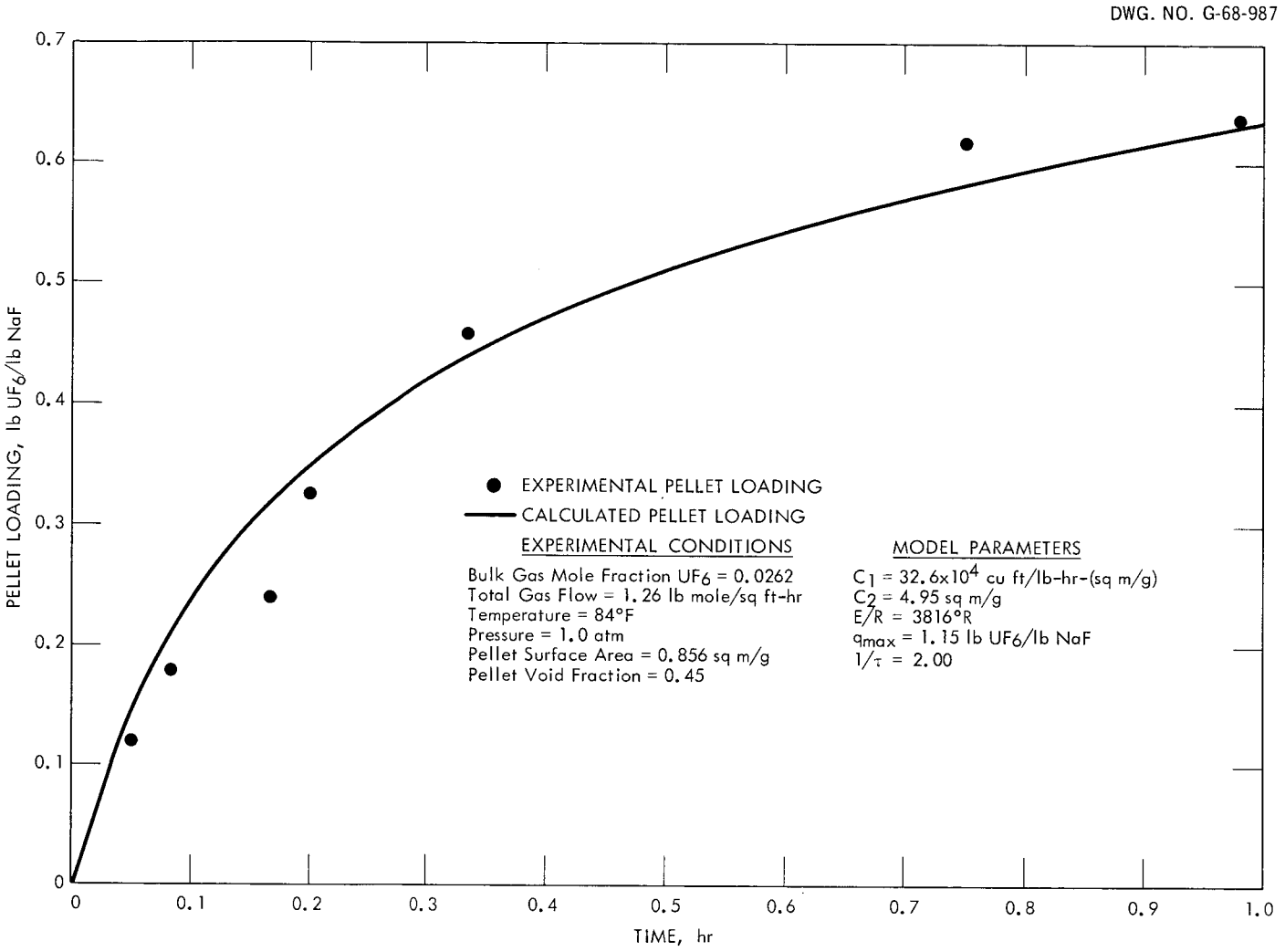

FIGURE 1

COMPARISON OF COMPUTED WITH EXPERIMENTAL DIFFERENTIAL BED LOADING AT 84°F AND 2.62 MOLE PERCENT URANIUM HEXAFLUORIDE

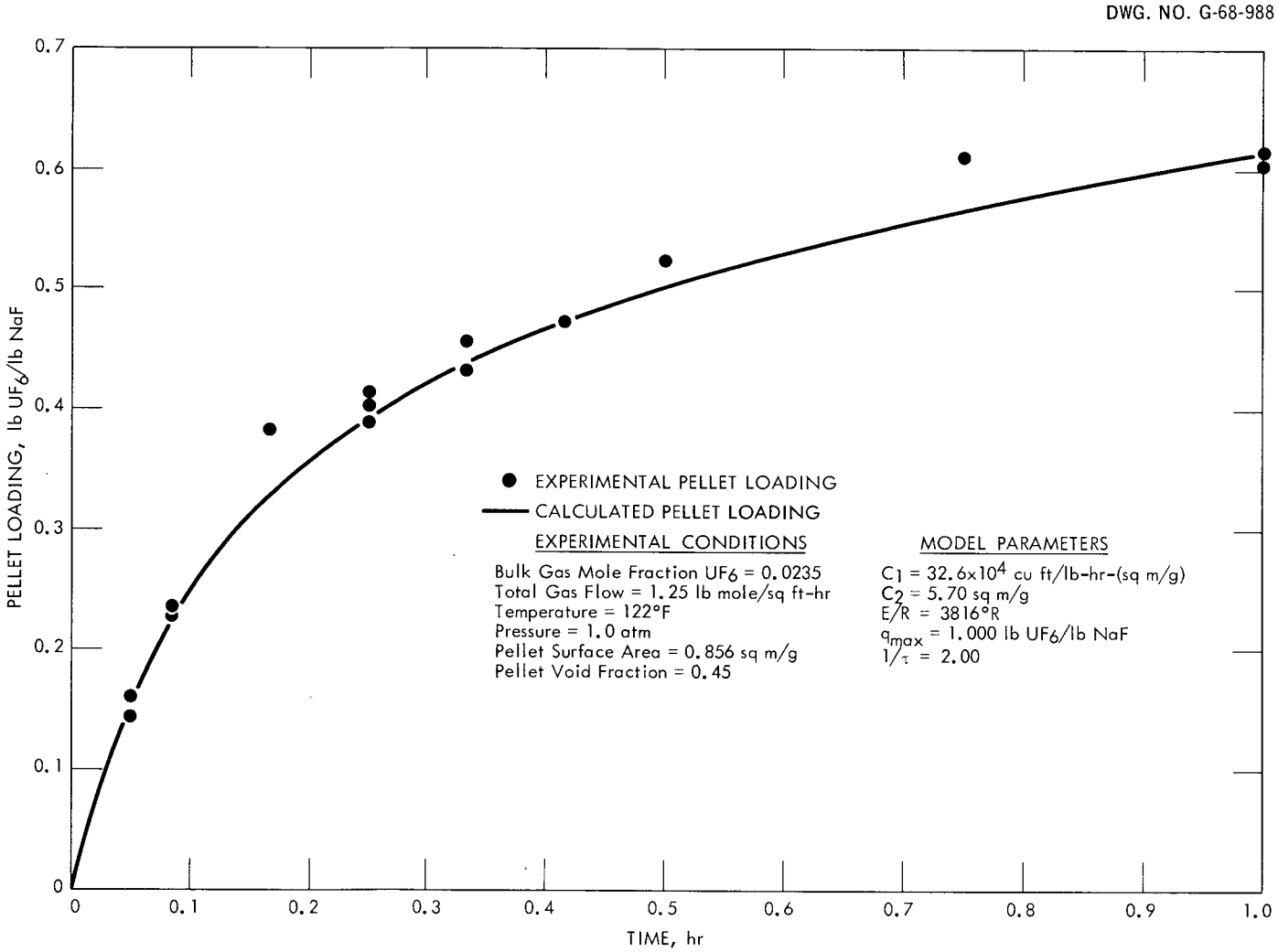

FIGURE 2

COMPARISON OF COMPUTED WITH EXPERIMENTAL DIFFERENTIAL BED LOADING AT 122°F AND 2.35 MOLE PERCENT URANIUM HEXAFLUORIDE

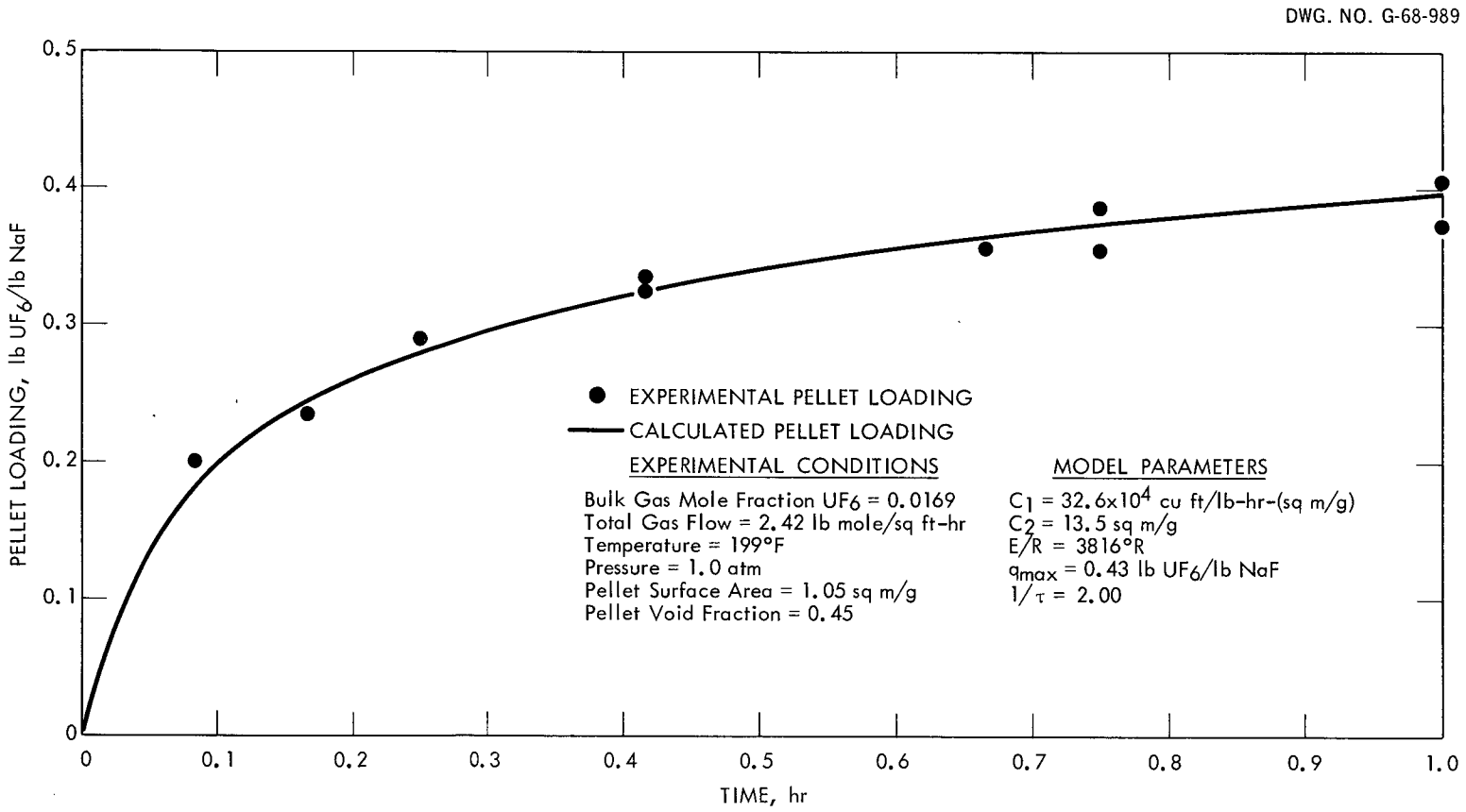

FIGURE 3

COMPARISON OF COMPUTED WITH EXPERIMENTAL DIFFERENTIAL BED LOADING AT 199°F AND 1.69 MOLE PERCENT URANIUM HEXAFLUORIDE

DWG. NO. G-68-990

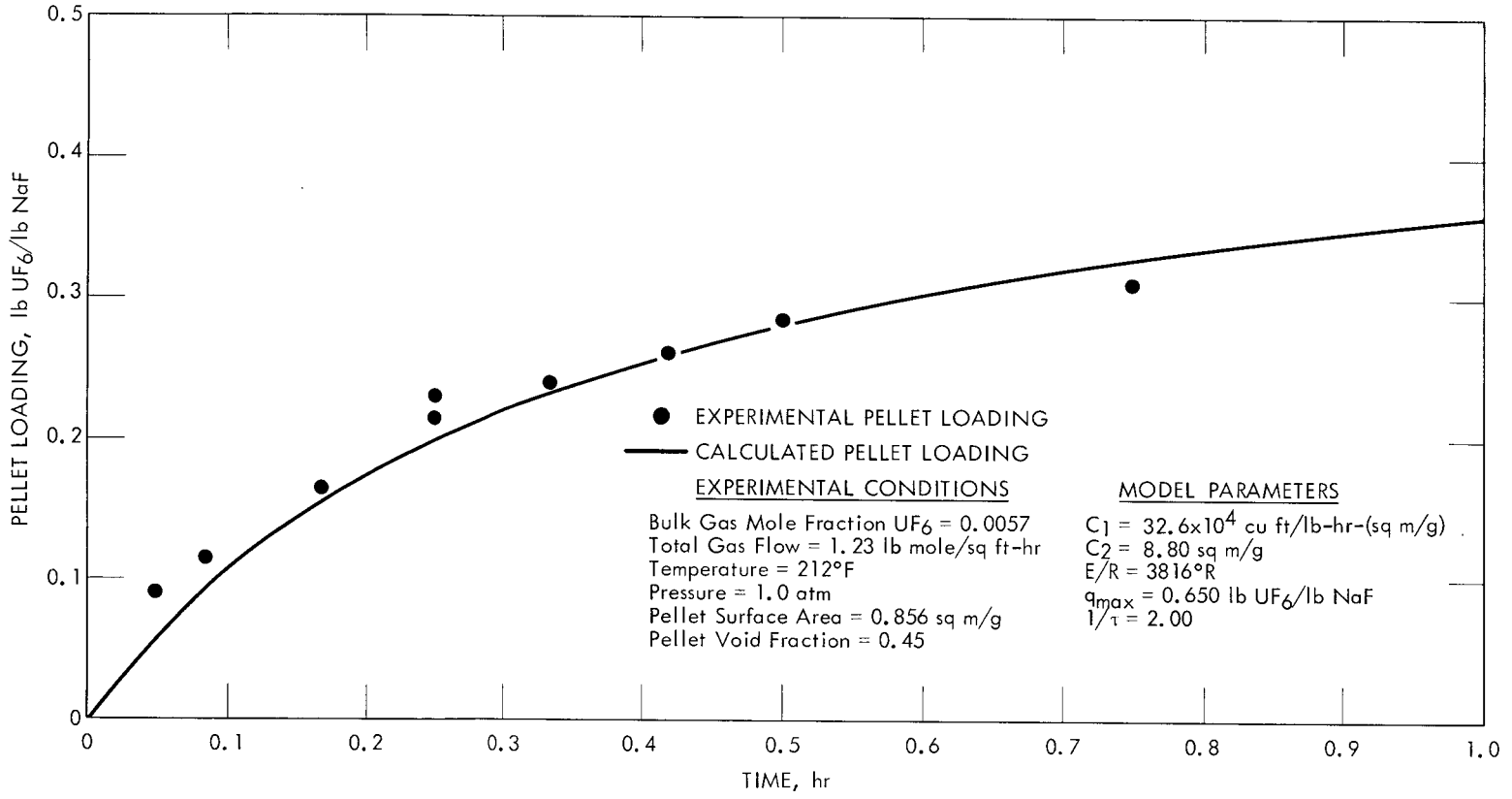

FIGURE 4

COMPARISON OF COMPUTED WITH EXPERIMENTAL DIFFERENTIAL BED LOADING AT 212°F AND 0.57 MOLE PERCENT URANIUM HEXAFLUORIDE

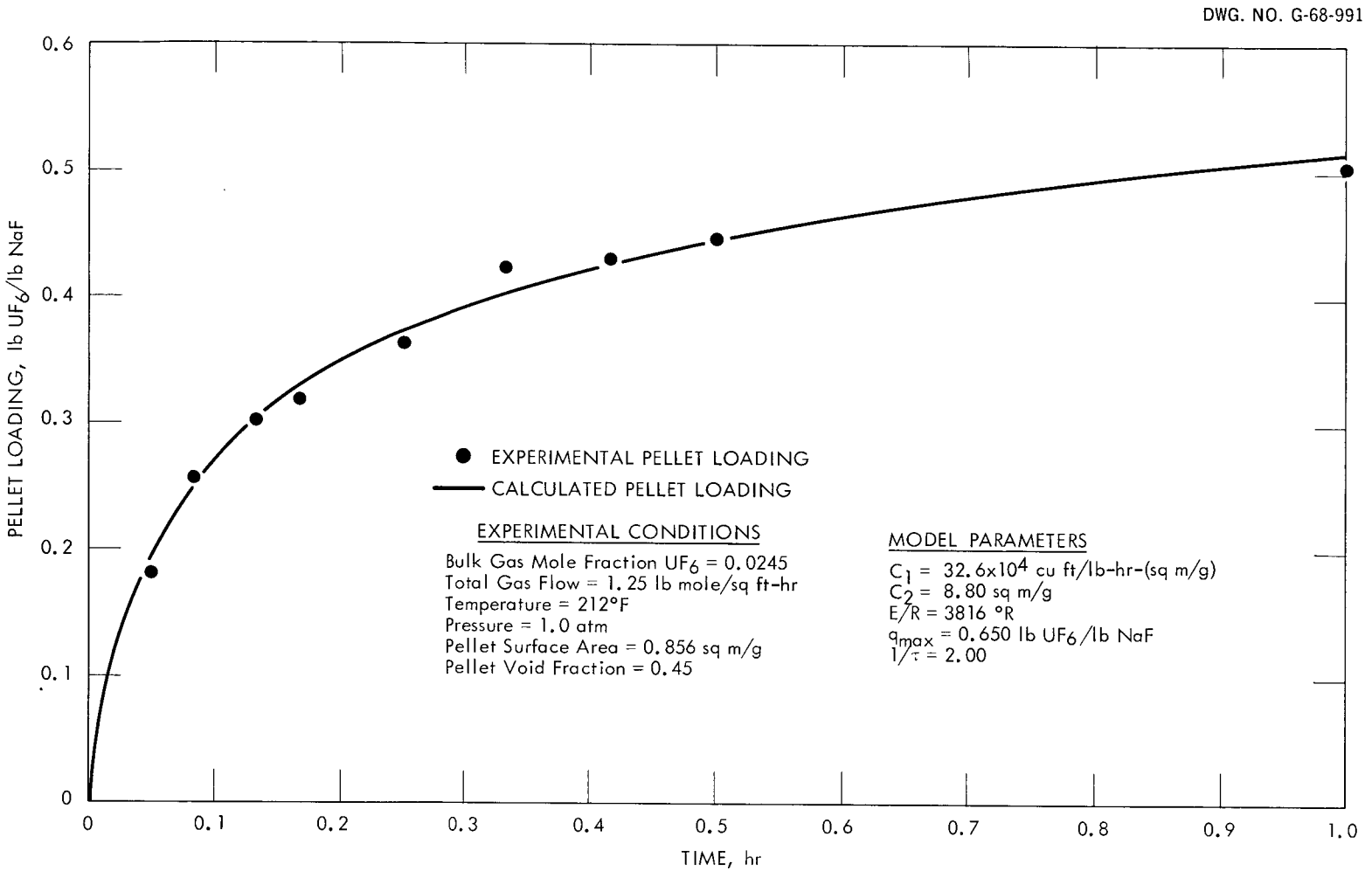

FIGURE 5

COMPARISON OF COMPUTED WITH EXPERIMENTAL DIFFERENTIAL BED LOADING AT 212°F AND 2.45 MOLE PERCENT URANIUM HEXAFLUORIDE

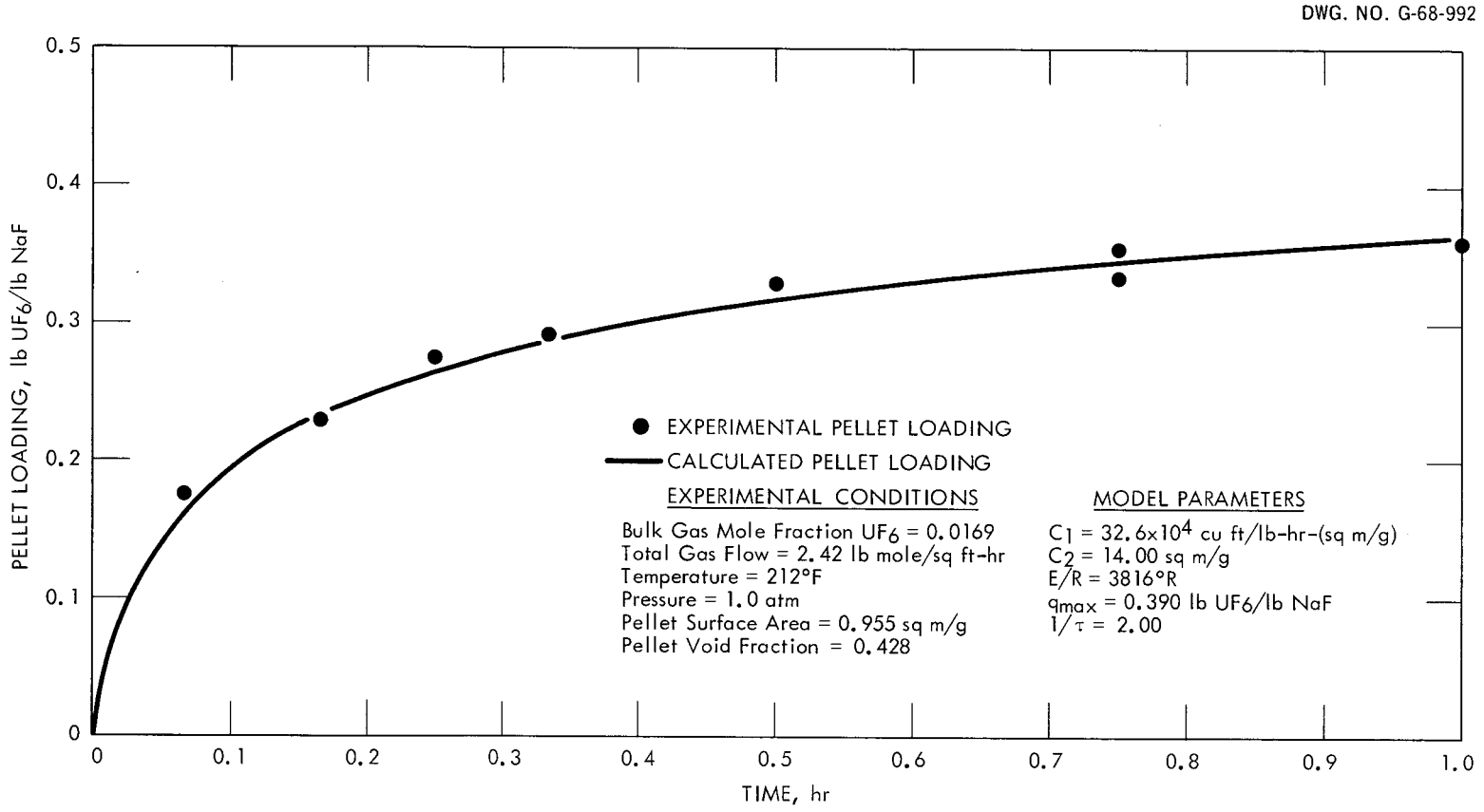

FIGURE 6

COMPARISON OF COMPUTED WITH EXPERIMENTAL DIFFERENTIAL BED LOADING AT 212°F, 1.69 MOLE PERCENT URANIUM HEXAFLUORIDE, AND 0.428 PELLET VOID FRACTION

DWG. NO. G-68-993

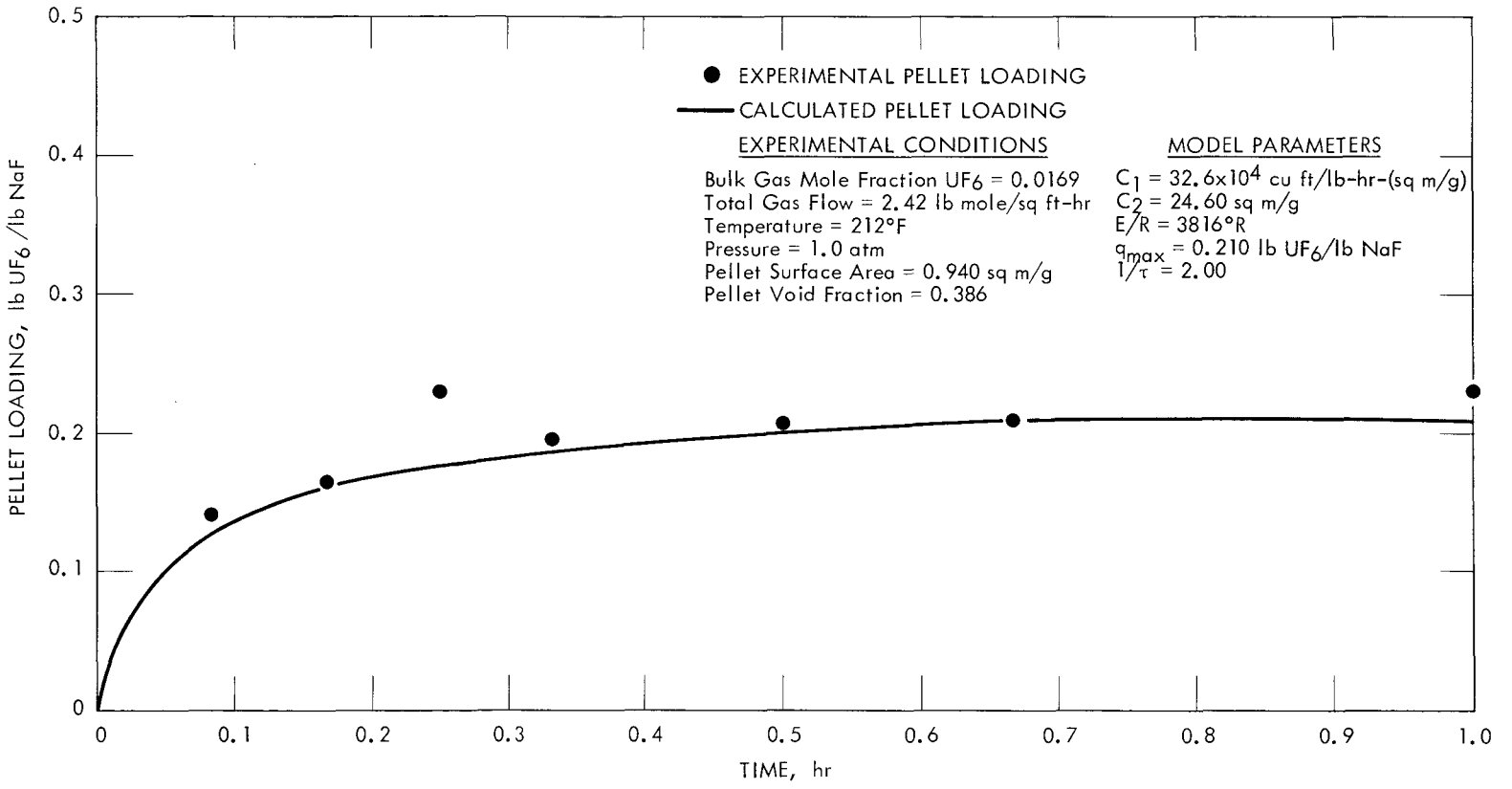

FIGURE 7

COMPARISON OF COMPUTED WITH EXPERIMENTAL DIFFERENTIAL BED LOADING AT 212°F, 1.69 MOLE PERCENT URANIUM HEXAFLUORIDE, AND 0.386 PELLET VOID FRACTION

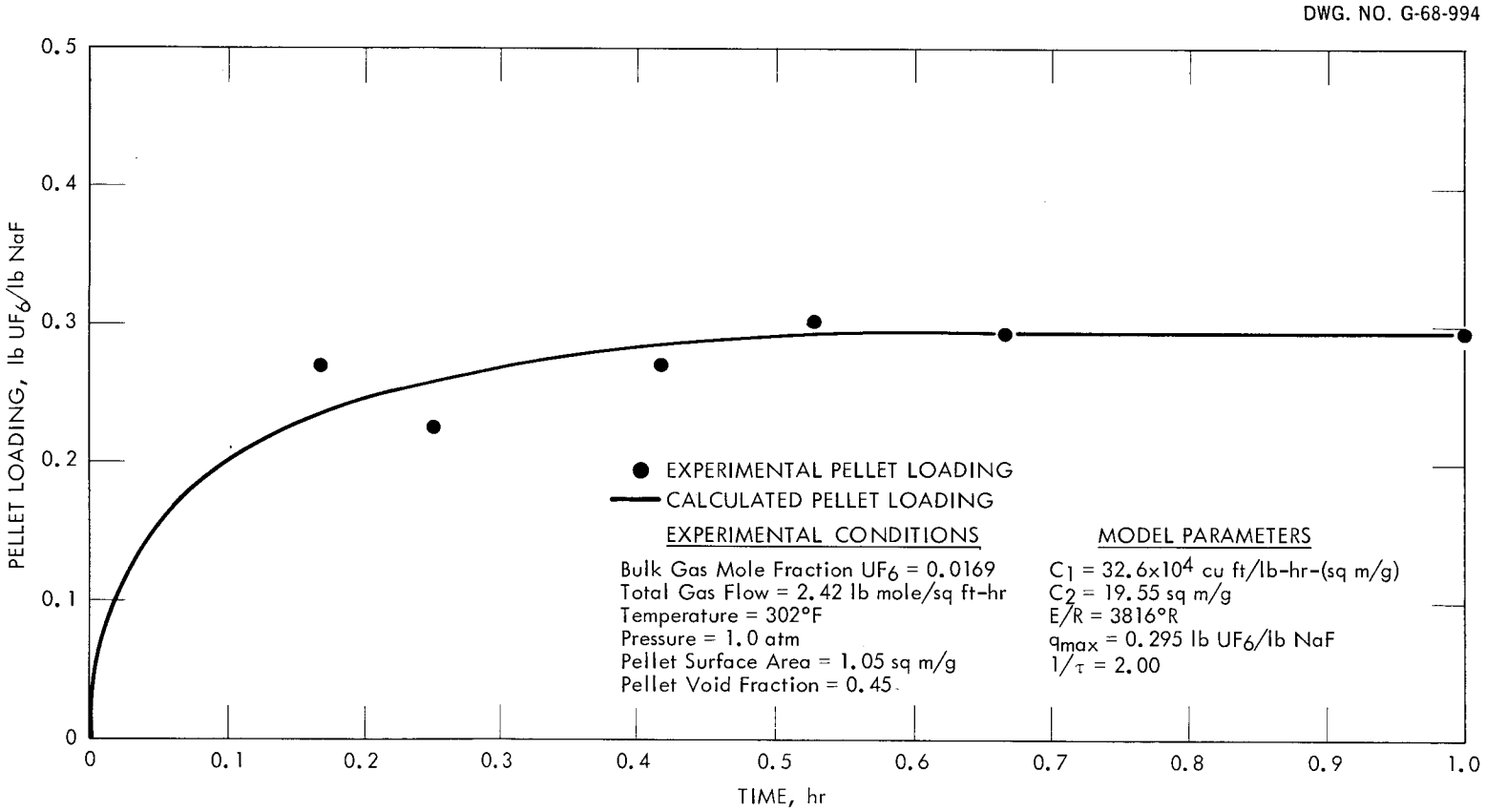

FIGURE 8

COMPARISON OF COMPUTED WITH EXPERIMENTAL DIFFERENTIAL BED LOADING AT 302°F AND 1.69 MOLE PERCENT URANIUM HEXAFLUORIDE

The value of $\overline{C}_2$ determines the rate at which the pellet adsorption rate decreases with the quantity of uranium complexed. The constant $\overline{C}_2$ was first independently determined for each different bed run and the values plotted to form the basis for the solid line shown in Figure 9. The $\overline{C}_2$ values were then adjusted to fall on this line, and it is these final values which are reported here and used in calculating the curves in Figures 1 through 8. It was apparent early in the investigation that $\overline{C}_2$ was some function of the effectiveness, or availability, of the internal pellet surfaces for reaction. A correlation with the maximum pellet loading appeared to be logical for $\overline{C}_2$, since both quantities tend to restrict the adsorption process. As demonstrated experimentally, the maximum loading of a sodium fluoride pellet increases as the porosity of the pellet increases, and the need of a porosity term in the correlation was, therefore, not at all surprising.

The mean free path of uranium hexafluoride in uranium hexafluoride-nitrogen mixtures in the temperature range of 84 to 212°F, concentration range of 0.5 to 8.5 mole percent uranium hexafluoride, and at atmospheric pressure has been reported to vary between 257 and 331 Å [17]. Since the initial average pore sizes of the sodium fluoride pellets were, in general, better than an order of magnitude larger than the mean free path of the diffusing molecules, only the bulk diffusion contribution to the effective diffusion coefficient was felt significant for this study. Furthermore, an ε dependence appeared to fit the data better than an ε^2 dependence in calculating the effective diffusion coefficient, thus dictating the use of Equation (12) rather than Equation (11) for D_{eff}. In

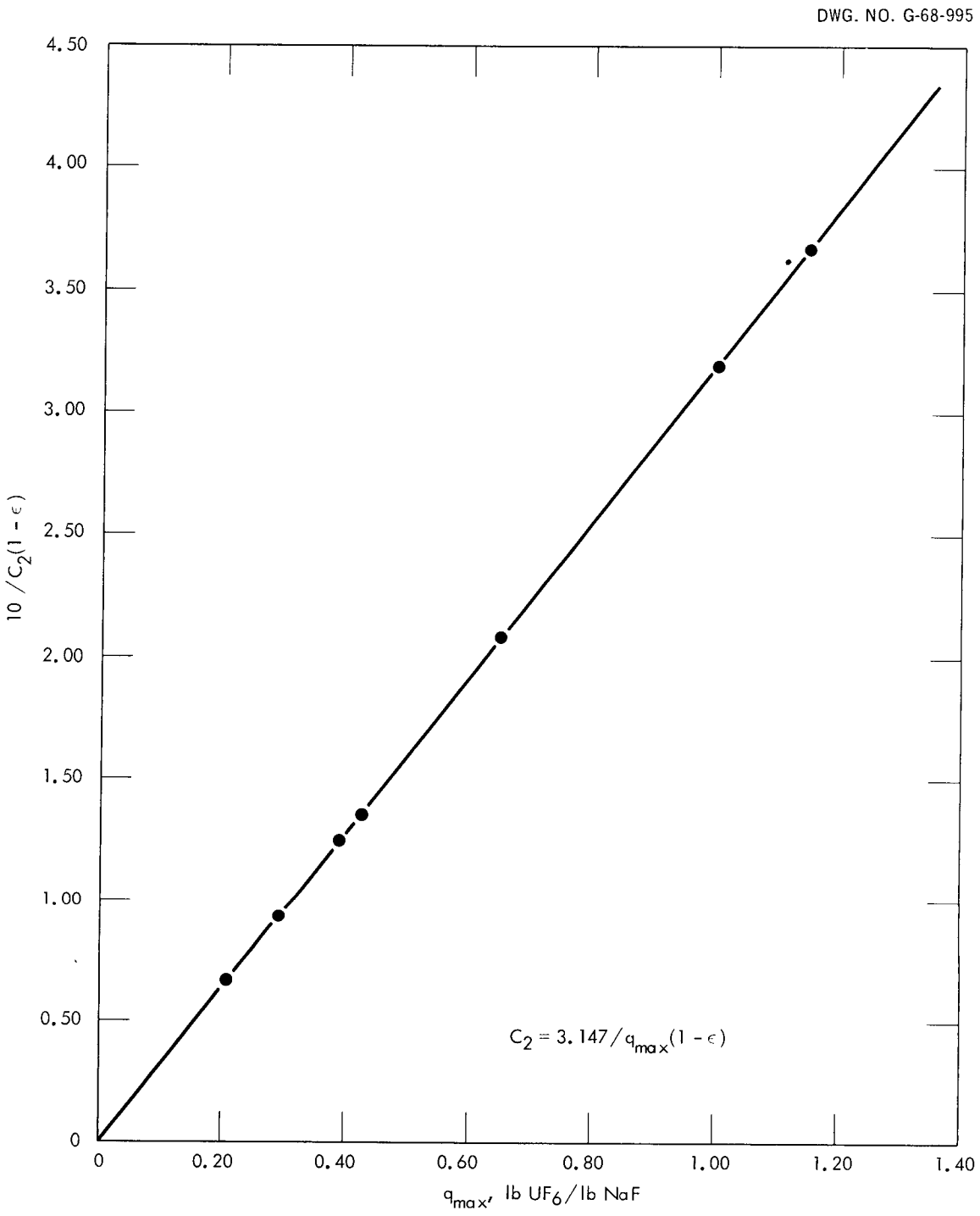

FIGURE 9

RELATIONSHIP OF REACTION RATE CONSTANT C_2 WITH MAXIMUM PELLET LOADING

considering values for the tortuosity factor τ, the choice seemed relatively arbitrary. A value of 0.5 was selected in agreement with those reported for porous materials with bimodal pore size distribution [20]. A listing of calculated bulk diffusion coefficients for the uranium hexafluoride-nitrogen binary system is given in Appendix B.

The magnitude of the effective mass transfer area was found to affect the initial pellet loading rate. After the first few minutes of adsorption, however, further influence was not apparent due to the evolution of a reaction rate controlled mechanism. The best value for the effective transfer area for the Harshaw pellets was found to be 0.0015 sq ft/pellet. Because of the apparent flexibility of the relation, the mass transfer correlation of Gupta and Thodos given by Equation (7) was incorporated into the model. Gas flow rates for the differential bed adsorption studies were typically low, with Reynolds numbers from 10 to 20.

CHAPTER V

COMPARISON OF RESULTS WITH EXPERIMENTAL FIXED-BED STUDIES

The deciding test of the proposed mathematical model describing the adsorption of uranium hexafluoride on sodium fluoride rests on a quantitative comparison of reported adsorber performance data and calculations using the model. At present, only a limited amount of fixed-bed performance data are available for the uranium hexafluoride-sodium fluoride system. These data, however, cover a broad area of typical trap operating conditions. The comparisons of five independent runs are presented in this chapter, demonstrating the strength of the overall analysis.

Fixed-Bed Breakthrough Data

Anderson [1] reports an experimental investigation of the adsorption of uranium hexafluoride on fixed beds of sodium fluoride pellets. The investigation was carried out to gain a better understanding of the dependence of the adsorption mechanism upon various physical parameters such as temperature, total gas flow rate, and pellet properties. In particular, pellet bed breakthrough and saturation characteristics were determined for a number of different operating conditions. The adsorption trap used in the study consisted of a vertical length of 4-inch-diameter nickel pipe, providing for a maximum 7-foot-deep bed of pellets. The trap was electrically heated and water cooled and was installed with a gas metering station, cold traps, and an outlet gas uranium

hexafluoride detection unit. Metering of the uranium hexafluoride was accomplished by maintaining a given forepressure and pressure drop across a calibrated capillary.

A typical run consisted of charging the pellet trap to a specified height, heating the bed to a desired temperature, establishing a diluent and uranium hexafluoride gas flow, and then valving the gas mixture through the pellet bed. Gas samples were withdrawn periodically from the inlet and outlet of the pellet bed and were analyzed during the run. The end result of each run was a concentration profile of the breakthrough curve as it emerged from the bed.

Adsorption temperatures of 200 and 250°F and a pressure of 1.14 atm are reported. Total gas flow rates varied from around 5 to 7 lb-mole/sq ft-hr and uranium hexafluoride inlet gas concentration ranged from 2.16 to 3.16 mole percent. Nitrogen was used as the diluent gas for all runs. Pellet properties varied widely, with surface areas of 0.924 to 1.94 sq m/g and void fractions of 0.436 to 0.55. Again, as was the case with the differential bed study, commercially available sodium fluoride pellets, manufactured by the Harshaw Chemical Company, were used. Complete details of the pellets are not presented here, but are readily available [17,22,23]. The wide variation of the pellet structure is typical of the commercially prepared pellets. Depending upon the desired bed heights, 20 to 40 pounds of pellets were used for each run. Anderson reports four runs with a 4-foot bed and one run with a 7-foot bed.

Results of the Comparison

Breakthrough curves were generated from the mathematical model using the specified physical parameters for each experimental run reported by Anderson. The curves are presented in Figures 10 through 14, along with the corresponding experimental data for comparison, and a convergence check on the numerical solution of the model equations is presented in Appendix D for a typical run. A time increment of 0.01 hour and bed increment of 0.05 foot were used for each of the runs.

On an overall basis, the results from the comparisons are very encouraging. The trap operating parameters and physical properties of the pellets used for the first four runs were similar to those used earlier in the determination of the rate reaction constants. One naturally would expect the model to be the strongest in this region, and this, in fact, appears to be the case. In each of these first four cases, the calculated break point agrees to within 0.1 hour of the experimental break point, and of equal importance, the calculated break profile compares very well with the reported data. The last run, however, indicates a possible overextension of the analysis, although unreported or undetected experimental difficulties could also be the problem. For this particular run, the pellets were found to have a surface area of 1.94 sq m/g and void fraction of 0.55. Normally, sodium fluoride pellets have surface areas from 0.7 to 1.4 sq m/g with void fractions between 0.37 to 0.50. Relatively high surface area pellets, i.e., pellets with surface areas greater than 1.8 to 1.9 sq m/g, are quite unusual, probably due to sintering in the one or more heat treatments required to harden

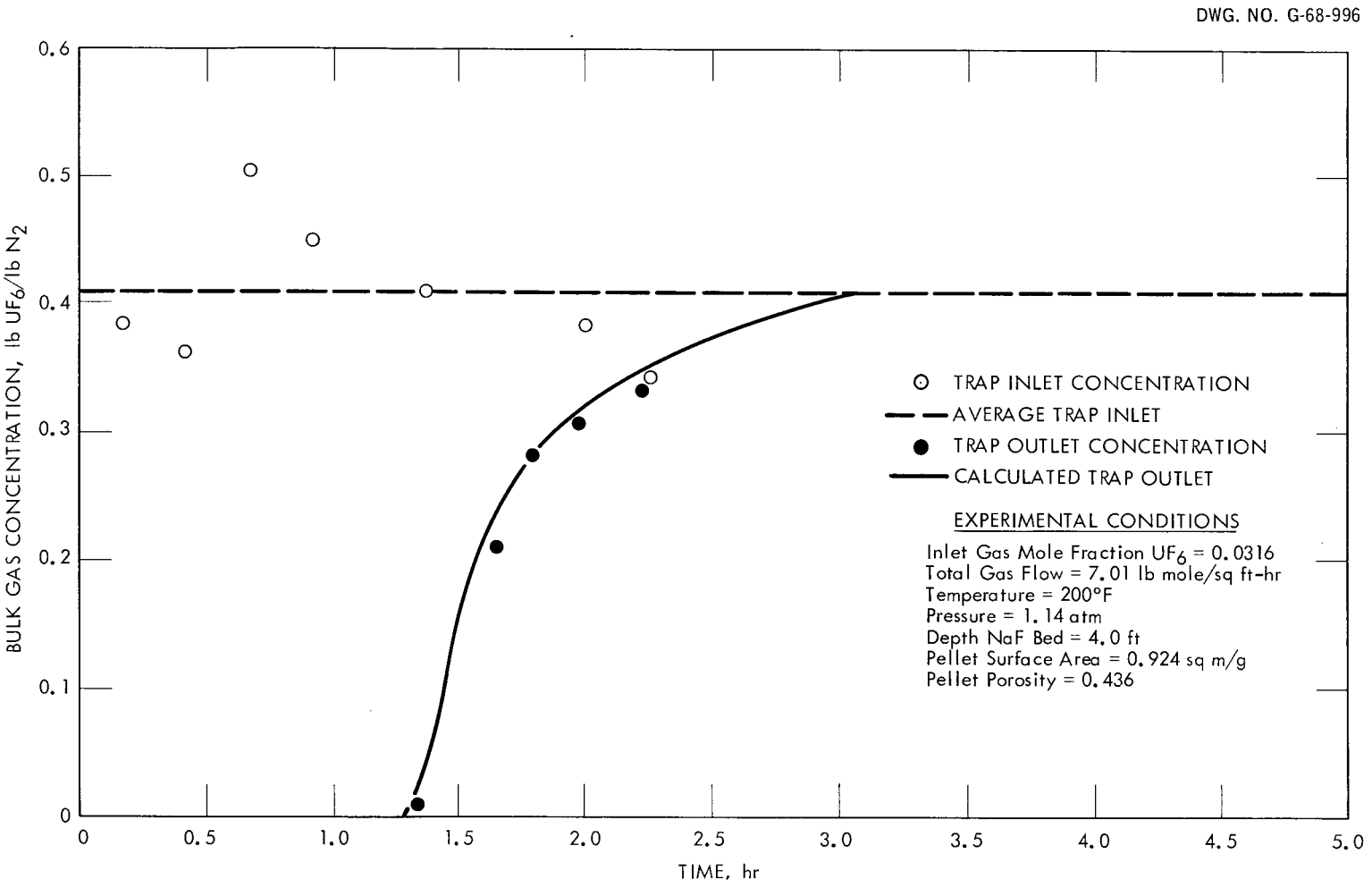

FIGURE 10

COMPARISON OF PREDICTED BREAKTHROUGH CURVES WITH EXPERIMENTAL DATA AT 200°F AND TOTAL GAS FLOW RATE OF 7.01 lb mole/sq ft-hr

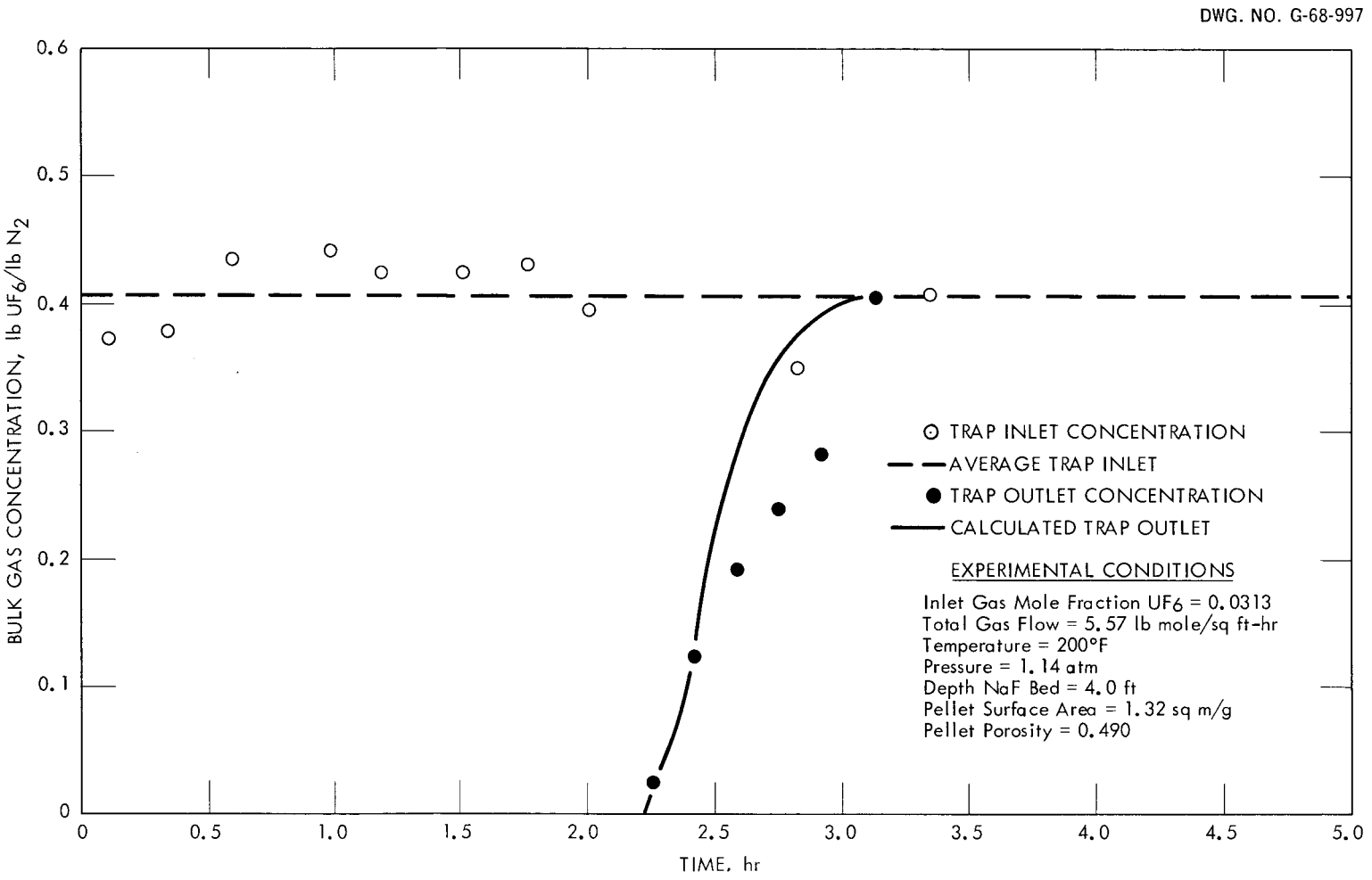

FIGURE 11

COMPARISON OF PREDICTED BREAKTHROUGH CURVES WITH EXPERIMENTAL DATA AT 200°F AND TOTAL GAS FLOW RATE OF 5.57 lb mole/sq ft-hr

DWG. NO. G-68-998

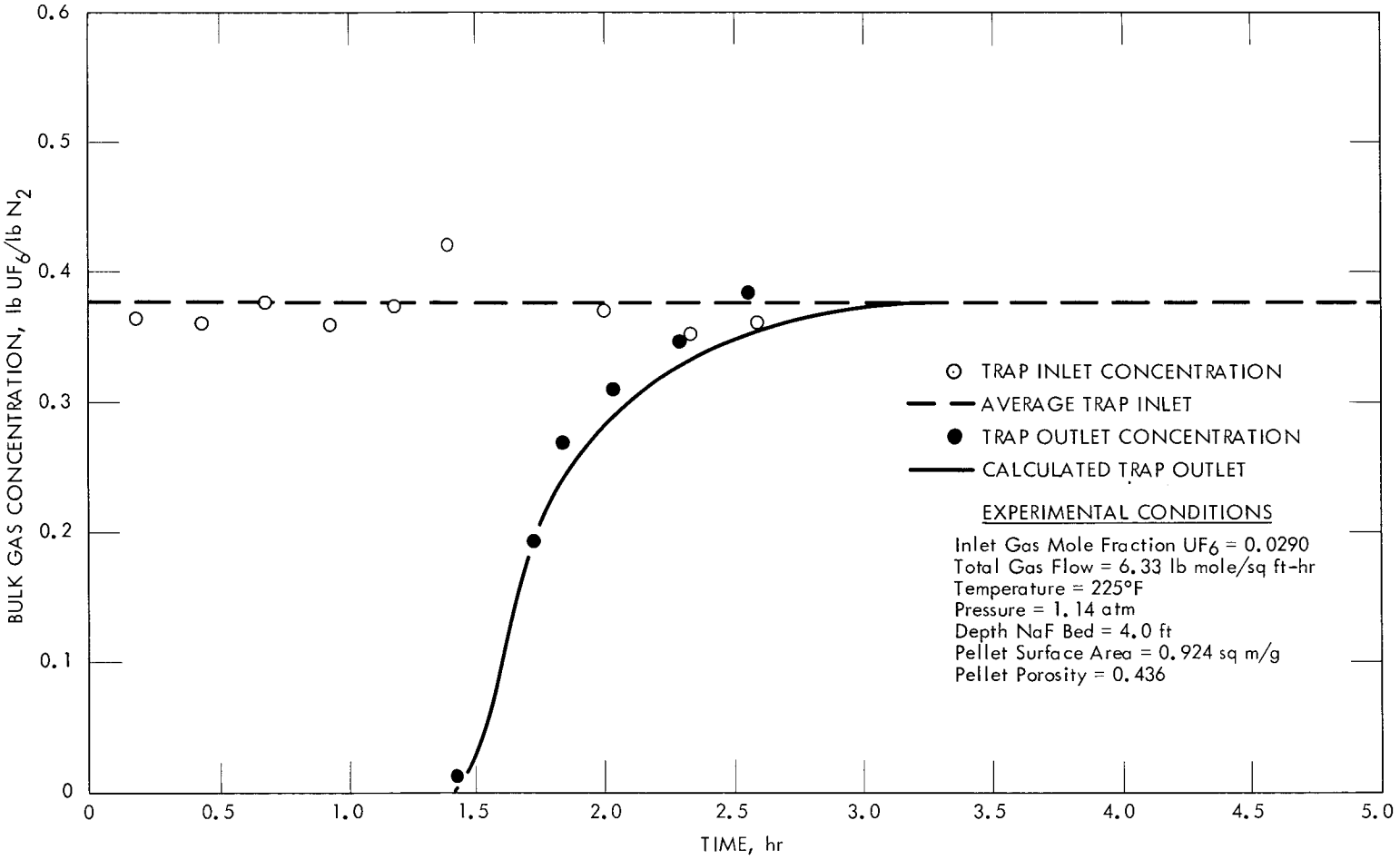

FIGURE 12

COMPARISON OF PREDICTED BREAKTHROUGH CURVES WITH EXPERIMENTAL DATA AT 225°F

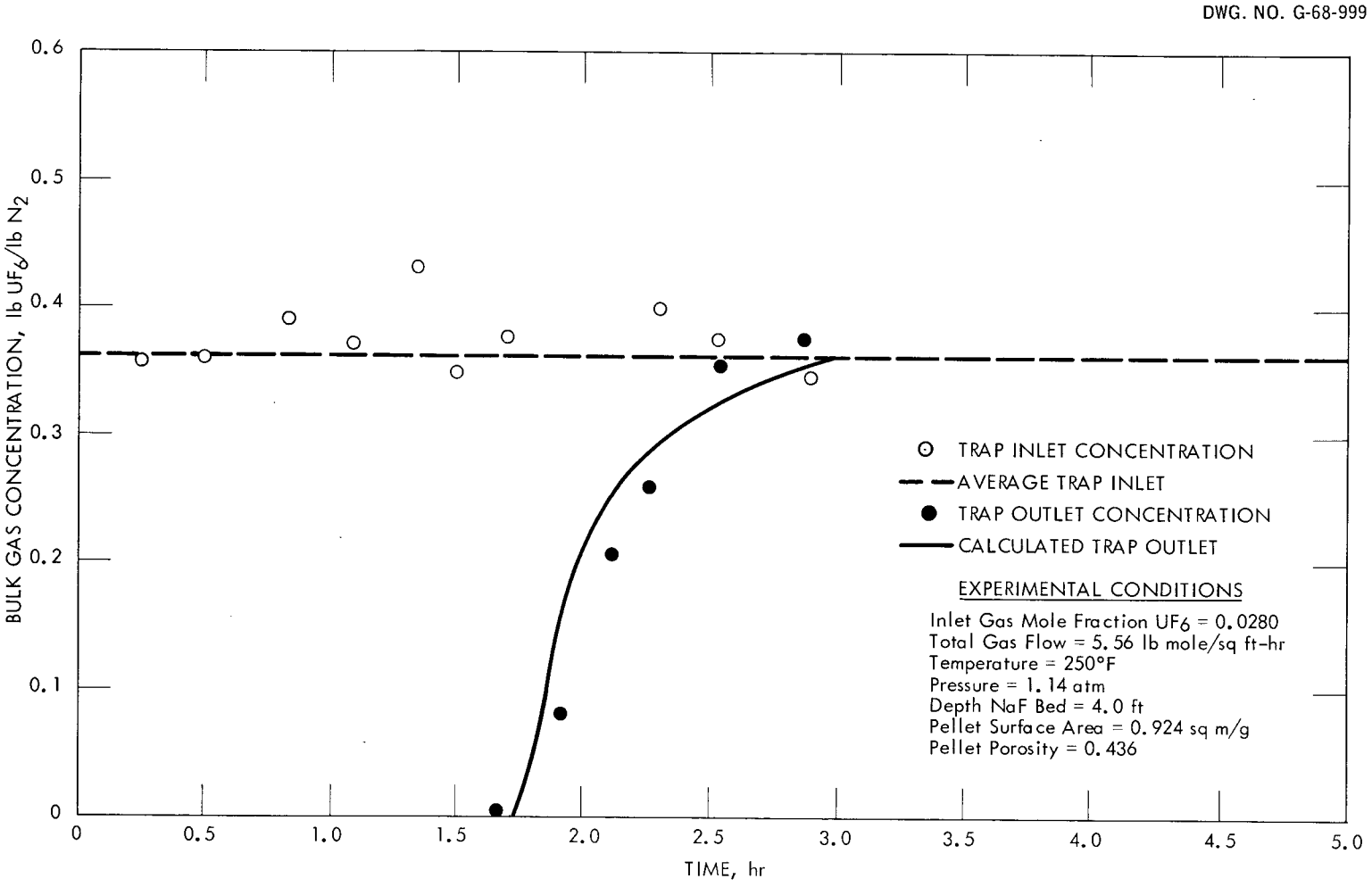

FIGURE 13

COMPARISON OF PREDICTED BREAKTHROUGH CURVES WITH EXPERIMENTAL DATA AT 250°F

DWG. NO. G-68-1000

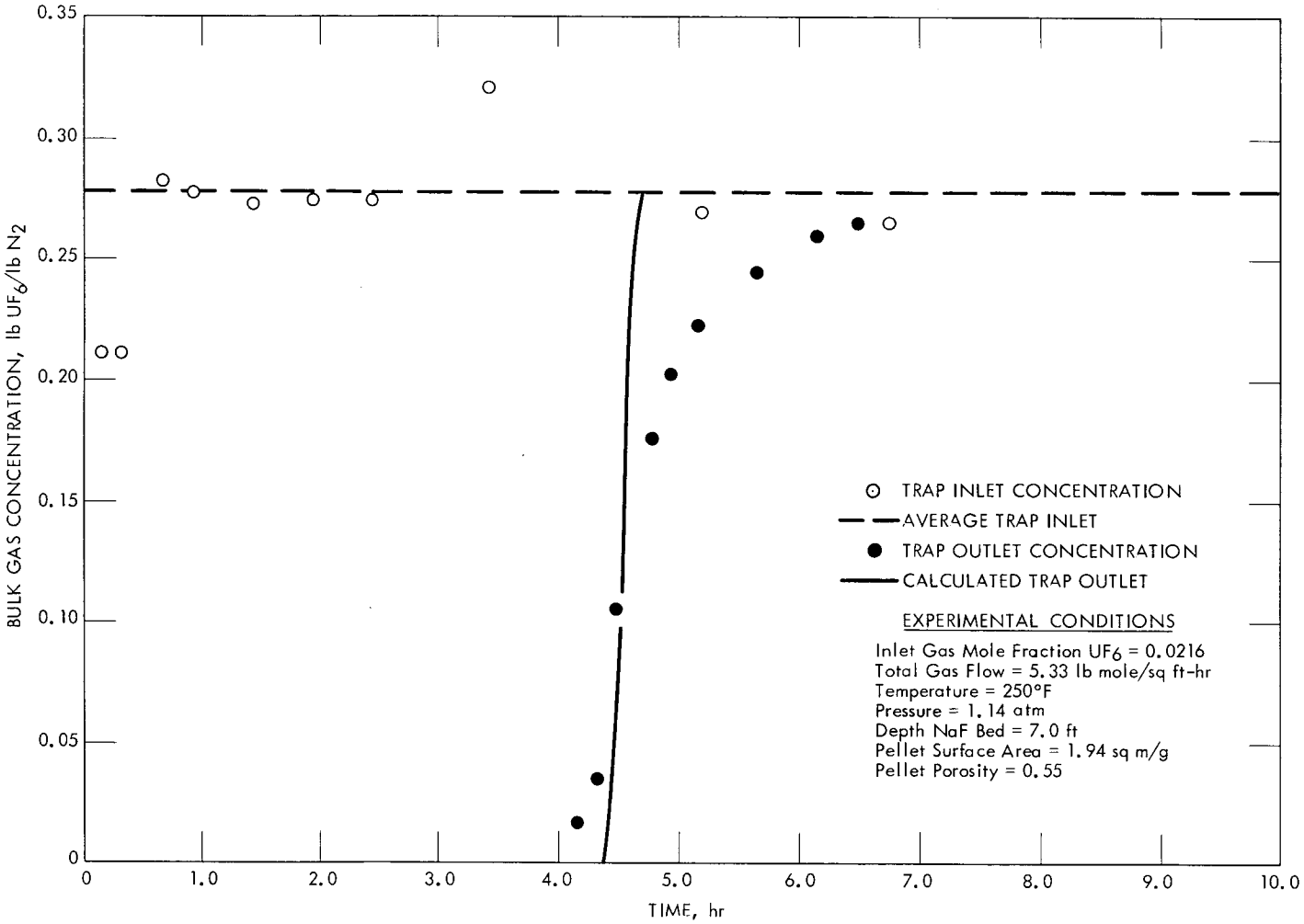

FIGURE 14

COMPARISON OF PREDICTED BREAKTHROUGH CURVES WITH EXPERIMENTAL DATA AT 250°F, USING HIGH SURFACE AREA PELLETS

and dry them after being formed. The choice of heat treatment temperature has been demonstrated to have a pronounced effect on the physical makeup of the pellets [22].

Because high surface area pellets are initially more active, the bulk of the reacting uranium hexafluoride should load quickly on the outer surfaces of the pellets, prematurely stopping further adsorption by blocking the passageways to the interior unreacted sodium fluoride. As a result, the pellets would be characterized by a low loading potential. With the relatively porous pellets considered here, however, the uranium loading is higher, and the pellets do not saturate rapidly. The model predicts that the pellets load quickly to saturation. The calculated adsorption zone, therefore, assumes a more or less plug form, with saturated pellets behind and fresh pellets in front, and consequently, the general shape of the calculated breakthrough curve shown in Figure 14 lacks the typical tail exhibited by the profiles of the preceding runs. Thus, the model apparently deviates somewhat from experimental results in this instance by not being able to adequately account for the high uranium hexafluoride loading capability of the high surface area pellets. Whether the deficiency lies in the assumption of the existance of an average pellet or in the correlation of the reaction rate constant $\overline{C}_2$, is speculation. The model does, however, reasonably establish the break point, which is the most important design criterion, and should, therefore, be sufficient until additional data become available to adequately define the problem area.

CHAPTER VI

DISCUSSION OF RESULTS

A mathematical model has been developed to aid in the sizing of fixed bed, sodium fluoride traps for the removal of uranium hexafluoride from an inert carrier gas. At present, the model is limited to isothermal, isobaric systems where the uranium concentration in the gas phase is limited to less than 10 mole percent. Operating temperatures should be below 300°F, with pressures around 1 to 2 atm. The model can accurately calculate the life and total uranium loading of a pellet trap, given a sufficient description of the physical system. Input specifications include the physical properties of the pellets, gas flow rate, inlet uranium hexafluoride concentration, operating temperature, and system pressure. Evidence supporting the analysis is presented in Chapter V.

The rate of removal of uranium hexafluoride from bulk gas flowing through a fixed bed of pelleted sodium fluoride has been found to be a function of the effective diffusion rate and surface concentration of the reacting uranium hexafluoride, the pseudo-first-order reaction rate constant for the uranium hexafluoride-sodium fluoride system, and the effective radii of the pellets. The overall rate increases with temperature and with pellet surface area, and decreases as the amount of uranium already complexed increases. The maximum loading of the pellet bed, i.e., pounds of uranium hexafluoride per pound of sodium fluoride,

decreases with increasing surface area, temperature, and pressure, and increases with pellet porosity. The maximum loading appears to be independent of the uranium content in the feed gas for gas concentrations of less than 8 to 9 mole percent. At higher concentrations, temperature gradients within the pellets can be expected to increase the effectiveness of the pellets and thereby increase their loading capacity.

Effects of Total Gas Flow and Concentration

The estimated dependence of bed height on total gas flow rate and uranium hexafluoride gas concentration is shown in Figure 15. The calculations were based on an operating temperature of 250°F and pressure of 1.36 atm. The pellets were assumed to have a surface area of 1.0 sq m/g and a porosity of 0.45. The quoted bed heights represent the trap lengths required for an on-stream time of 24 hours, with the indicated feed concentrations and total gas flow rates. Breakthrough was taken as the time when the concentration of uranium hexafluoride in the adsorber off-gas exceeded that associated with the equilibrium decomposition pressure of the complex. In actual operation, at 250°F, the off-gas will typically contain from 20 to 30 ppm uranium hexafluoride within a short time after being put on-stream. The detection of the equilibrium concentration does not constitute the break point. Depending upon the operating conditions of the particular system, the adsorption zone may be only a few minutes, a few hours, or even longer, behind the equilibrium front.

Caution should be exercised in extrapolation of the results to higher flows because the curves, although not shown here, eventually break upward. Excluding the initial contact with the pellet, diffusion

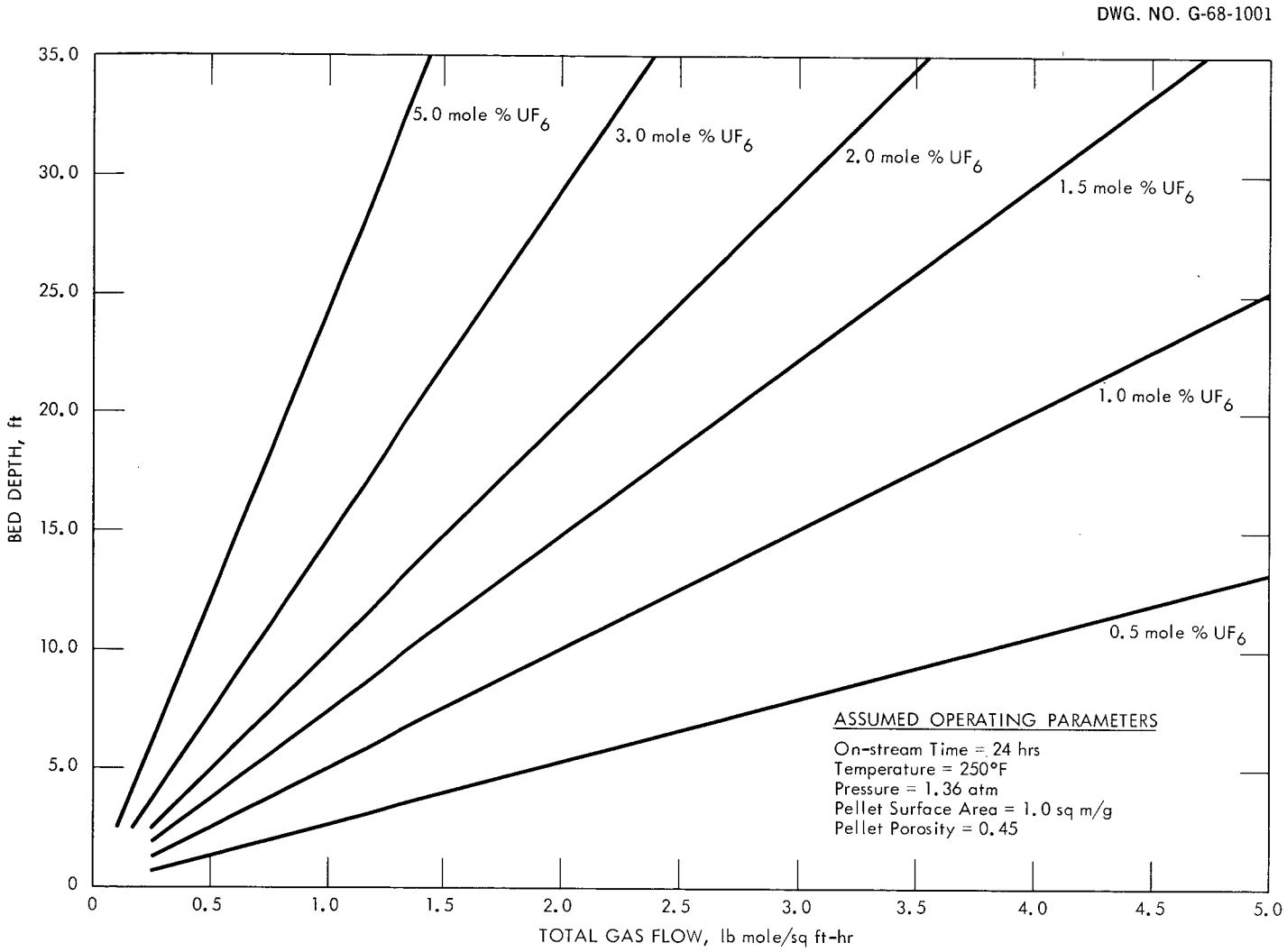

FIGURE 15

REQUIRED PELLET BED DEPTH AS A FUNCTION OF TOTAL GAS FLOW RATE AND URANIUM CONCENTRATION AT 250°F

of the reacting uranium hexafluoride from the bulk gas to the surface of the pellet is not rate controlling. Consequently, the rate of adsorption is essentially independent of mass flow rate.

Effect of Temperature

The effect of lowering the operating temperature of the sodium fluoride bed is shown in Figure 16, where the cases summarized in Figure 15 are repeated at a lower temperature, 200°F. At the lower temperature, the reacting molecules are allowed to diffuse deeper into the pellets before becoming immobilized because the pellets are somewhat less active. Since more of the pellet is made available for reaction, higher loadings result. Consequently, lower operating temperatures generally result in smaller trap requirements. For example, comparing Figures 15 and 16 for the two cases where 2.0 lb mole/sq ft-hr of feed containing 1.5 mole percent uranium hexafluoride are fed, trap heights of 14.8 feet for the 250°F case and 10.7 feet for the 200°F case are obtained. Again, caution must be used in extrapolating the curves to higher flows. A disadvantage in operating at the lower temperature lies in the decreased adsorption rate, which is an important consideration at higher flows and for instances where low surface area pellets are used.

Effect of Pellet Surface Area

Realizing that the surface area of the reacting pellets plays an important role in the definition of trap performance, a number of calculations were made to determine the effect of varying pellet surface area on trap height. The results are shown in Figure 17. For these

DWG. NO. G-68-1002

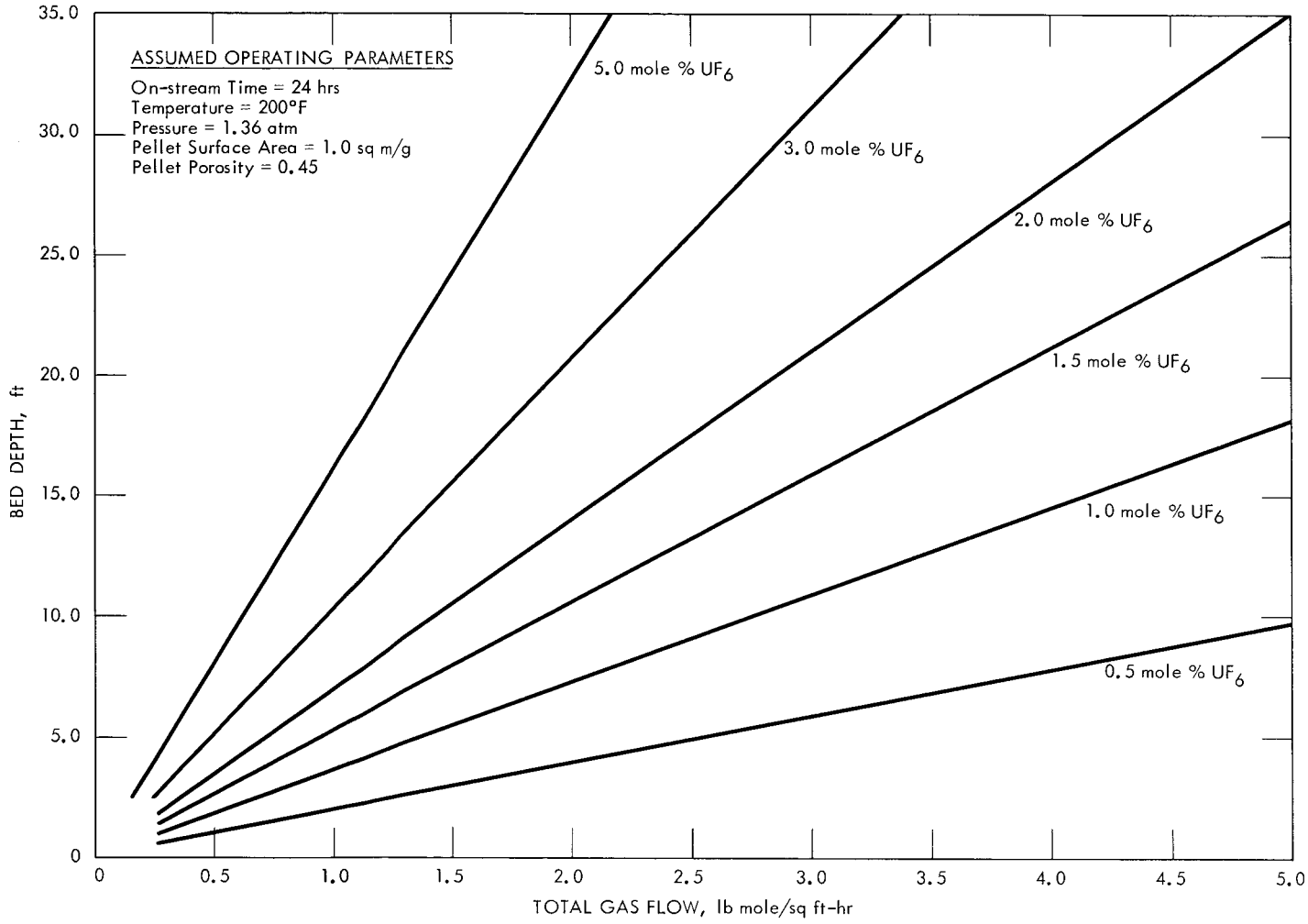

FIGURE 16

REQUIRED PELLET BED DEPTH AS A FUNCTION OF TOTAL GAS FLOW RATE AND URANIUM CONCENTRATION AT 200°F

DWG. NO. G-68-1003

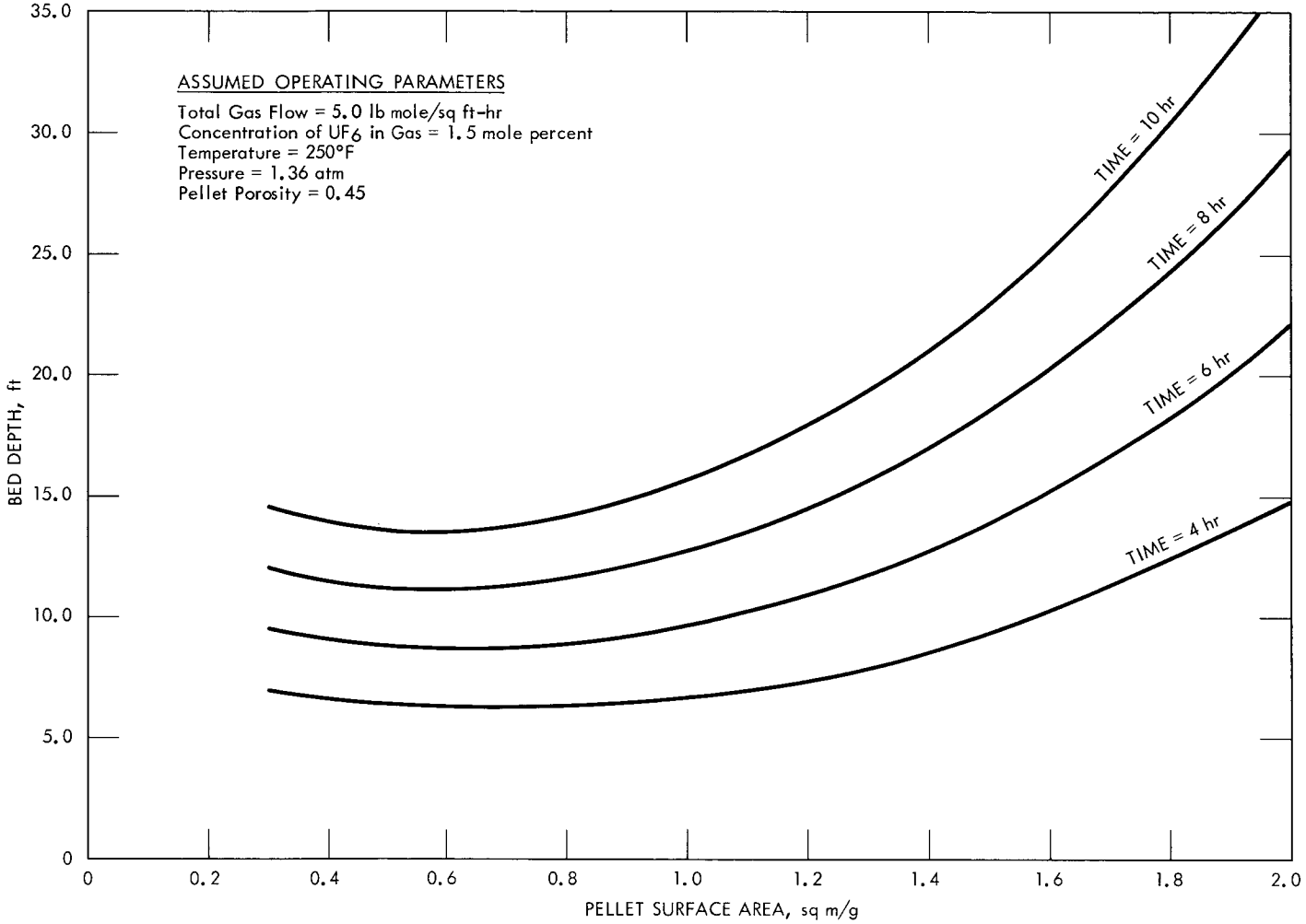

FIGURE 17

REQUIRED PELLET BED DEPTH AS A FUNCTION OF PELLET SURFACE AREA AND ON-STREAM TIME

determinations, the trap temperature was maintained at 250°F, the pressure was held at 1.36 atm, and the total gas flow rate was set at 5.0 lb mole/sq ft-hr. The porosity of all pellets was assumed to be 0.45. Results are given for breakthrough times of 4 to 10 hours.

High surface area pellets are more reactive than pellets with less surface. For the more reactive pellets, as discussed in Chapter V, the bulk of the uranium hexafluoride loads quickly on the periphery. The length of the adsorption zone in such instances is generally short, and the required length of trap depends primarily upon the loading capabilities of each bed segment. As surface area is lowered, the pellets are rendered less active and, hence, the loading potential increases because more of the internal pellet surfaces become available for reaction. For the less active pellets, the kinetics of the process begin to play an increasingly important role in trap sizing by off-setting the gains offered by the higher loading. Eventually, a point of diminishing returns is reached where the loss of reactivity completely overshadows the loading gain, and trap requirements begin to increase with further decrease in pellet reactivity.

As demonstrated in Figure 17, for the cases studied, an apparent optimum surface area exists around 0.6 to 0.8 sq m/g. The minimum point does, of course, depend upon the mass flow rate. For higher flows, the minimum should move toward increasing surface area. In setting pellet specifications, other factors such as the number of cycles of useful pellet life must also be considered. Reactive, high surface area pellets are relatively soft in most cases and tend to crumble and powder as

adsorption and desorption steps are carried out [22]. However, some surface degradation is unavoidable, regardless of the physical condition of the pellets, because of the differences in crystalline density of sodium fluoride and the $UF_6 \cdot 2NaF$ complex. Being formed in a state of lateral compression, the newly formed complex exerts a tendency to buckle and slough from the underlying sodium fluoride.

Adsorber Operation

In general practice, a series trap arrangement is recommended over a parallel one for adsorption cases where the length of the adsorption zone is large relative to the length of the pellet bed. Here, when breakthrough occurs, the pellet bed would not be saturated, and substantial loading potential would be lost if the trap were removed from service. By valving in a fresh trap downstream of the partially spent one and allowing the first trap to remain in service until fully saturated, the total loading of the pellet bed can, in such instances, be substantially increased. On the other hand, little advantage would be gained by operating traps in series when the adsorption zone is small, because the bed would be essentially saturated at breakthrough. From an economic point of view, considering the time to change out and regenerate the sodium fluoride traps, pumping and heating costs, and pellet life, proper operation of traps usually proves worthwhile.

The length of the adsorption zone for the uranium hexafluoride-sodium fluoride system is a function of many parameters. Considering the cases where the sodium fluoride trap is operated at higher temperatures and pressures, say 250°F and 1.34 atm, with pellets having surface

areas of 1.0 sq m/g or greater, and where the feed material contains at least 0.5 mole percent uranium and is supplied at rates less than 4.0 to 5.0 lb mole/sq ft-hr, the resulting adsorption zone becomes short, generally less than 3 feet. For cases where less reactive pellets, e.g., pellets with surface areas less than 0.8 sq m/g, are used with feed material containing less than 1.0 mole percent uranium at flow rates greater than 5.0 lb mole/sq ft-hr, the adsorption zone becomes relatively large, being better than 5 to 10 feet long.

Determination of the Maximum Pellet Loading

The use of the described model requires a knowledge of the maximum loading of uranium hexafluoride on the particular sodium fluoride pellets to be used. As previously mentioned, the maximum loading decreases with increasing surface area, temperature, and pressure, and increases with pellet porosity. The most accurate method of obtaining the loading value is, of course, by actual experimentation. A mathematical model developed by McNeese [17] to describe the adsorption of uranium hexafluoride by a single pellet of sodium fluoride is currently available to predict loading capacities. By knowing the surface area, porosity, and temperature, maximum loading values can be estimated from the general results of McNeese's program given in Appendix E. A preliminary correlation between the maximum pellet loading and the effectiveness of the pellet, as defined by the introduction of an effectiveness factor [4,21,27], has been obtained in the course of this work, but is not presented here because of the lack of experimental data needed to extend the scope of the correlation to a wider range of physical conditions.

CHAPTER VII

CONCLUSIONS AND RECOMMENDATIONS

Conclusions

From the results of this investigation, the following conclusions are made:

1. A mathematical model has been developed that can describe the dynamic adsorption of uranium hexafluoride on fixed beds of sodium fluoride from the physical parameters of the system.
2. The model can be used confidently as a tool for the design engineer to size sodium fluoride traps for use in uranium hexafluoride collection and purification.
3. Application of the model is limited to isothermal, isobaric adsorber systems where the uranium concentration in the gas phase is limited to less than 10 mole percent. Operating temperatures should be below 300°F with pressures around 1 to 2 atm.
4. Adsorber behavior is sensitive enough to properties of the sorbent that even variations normally present between batches of commercial pellets may significantly alter performance.

Recommendations

For further expansion of this investigation, the following recommendations are made:

1. Expand the applicability of the model to regions of lower operating pressures and higher temperatures.
2. Repeat the analysis using a diluent gas other than nitrogen, i.e., helium or argon.
3. Adapt the model to other systems of interest [23] similar to the one under study, e.g., the volatile metal fluorides of niobium, tantalum, antimony, ruthenium, and titanium that form complexes with solid sorbents, such as sodium fluoride, magnesium fluoride, and aluminum fluoride.
4. Develop the model of a multicomponent adsorption system, such as uranium hexafluoride and niobium pentafluoride on sodium fluoride, or uranium hexafluoride and titanium tetrafluoride on aluminum fluoride, in which the removal of volatile metallic impurities from uranium hexafluoride by selective adsorption on solid sorbents has been proposed [23].

LIST OF REFERENCES

LIST OF REFERENCES

1. Anderson, L. W., "An Experimental Investigation of the Adsorption of Uranium Hexafluoride on Fixed Beds of Sodium Fluoride," K-L-6221, Oak Ridge, Tennessee, Oak Ridge Gaseous Diffusion Plant, Union Carbide Corporation, Nuclear Division (Sept. 19, 1968).

2. Arnold, E. D., Barton, J. C., Keller, E. L., Levin, R. W., and Voss, F. S., Editors, "Uranium Hexafluoride Specification Studies," ORO-656, Oak Ridge, Tennessee, Oak Ridge Operations Office, United States Atomic Energy Commission (July, 1967).

3. Astarita, G., "Mass Transfer with Chemical Reaction," pp. 39-42, Elsevier Publishing Company, New York (1967).

4. Bird, R. B., Stewart, W. E., and Lightfoot, E. N., "Transport Phenomena," pp. 542-546, John Wiley and Sons, Inc., New York (1960).

5. Bradshaw, R. D., and Myers, J. E., "Heat and Mass Transfer in Fixed and Fluidized Beds of Large Particles", A.I.Ch.E.J. *9*, 590-595 (1963).

6. Cathers, G. I., Bennett, M. R., and Jolley, R. L., "$UF_6 \cdot 2NaF$ Complex Formation and Decomposition", Ind. Eng. Chem. *50*, 1709-1712 (1958).

7. Crank, J., "Diffusion with Rapid Irreversible Immobilization", Trans. Faraday Soc. *53*, 1083-1091 (1957).

8. DeMarcus, W. C., and Starnes, M. P., "The Intermolecular Interaction of Uranium Hexafluoride Molecules," K-1114, Oak Ridge, Tennessee, Oak Ridge Gaseous Diffusion Plant, Union Carbide Corporation, Nuclear Division (1954).

9. DeWitt, R., "Uranium Hexafluoride: A Study of the Physico-Chemical Properties," GAT-280, Portsmouth, Ohio, Portsmouth Gaseous Diffusion Plant, Goodyear Atomic Corporation (1960).

10. Dunthorn, D. I., Personal Communication, Oak Ridge, Tennessee, Oak Ridge Gaseous Diffusion Plant, Union Carbide Corporation, Nuclear Division.

11. Foust, A. S., Wenzel, L. A., Clump, C. W., Maus, L., and Anderson, L. B., "Principles of Unit Operations," pp. 208-212, John Wiley and Sons, Inc., New York (1960).

12. Gamson, B. W., "Heat and Mass Transfer," Chem. Engr. Prog. *47*, 19-28 (1951).

13. Gupta, A. S., and Thodos, G., "Mass and Heat Transfer in the Flow of Fluids Through Fixed and Fluidized Beds of Spherical Particles," A.I.Ch.E.J. *8*, 608-610 (1962).

14. Hougen, O. A., and Watson, K. M., "Chemical Process Principles," pp. 1080-1082, John Wiley and Sons, Inc., New York (1947).

15. Katz, S., "Use of High-Surface-Area Sodium Fluoride to Prepare $MF_6 \cdot 2NaF$ Complex with Uranium, Tungsten, and Molybdenum Hexafluorides," Inorg. Chem. *3*, 1598-1600 (1964).

16. Katz, S., "Preparation of $MF_6 \cdot NaF$ Complexes with Uranium, Tungsten, and Molybdenum Hexafluorides," Inorg. Chem. *5*, 666-668 (1966).

17. McNeese, L. E., "An Experimental Study of Sorption of Uranium Hexafluoride by Sodium Fluoride Pellets and a Mathematical Analysis of Diffusion with Simultaneous Reaction," ORNL-3494, Oak Ridge, Tennessee, Oak Ridge National Laboratory, Union Carbide Corporation, Nuclear Division (November, 1963).

18. Mickley, H. S., Sherwood, T. K., and Reed, C. E., "Applied Mathematics in Chemical Engineering," pp. 193-194, McGraw-Hill Book Company, Inc., New York (1957).

19. Perry, J. H., "Chemical Engineer's Handbook," Third Edition, p. 370, McGraw-Hill Book Company, Inc., New York (1950).

20. Reid, R. C., and Sherwood, T. K., "The Properties of Gases and Liquids," pp. 182-299, McGraw-Hill Book Company, Inc., New York (1958).

21. Satterfield, C. N., and Sherwood, T. K., "The Role of Diffusion in Catalysis," pp 12-26, Addison-Wesley Publishing Company, Inc., Reading, Massachusetts (1963).

22. Smiley, S. H., Brater, D. C., and Pashley, J. H., "ORGDP Fuel Reprocessing Studies, Summary Progress Report, Fiscal Year 1964 through Fiscal Year 1965," K-1649, Oak Ridge, Tennessee, Oak Ridge Gaseous Diffusion Plant, Union Carbide Corporation, Nuclear Division (October, 1965).

23. Stephenson, M. J., Merriman, J. R., and Kaufman, H. L., "Removal of Impurities from Uranium Hexafluoride by Selective Sorption Techniques: Progress Report for 1966," K-1713, Oak Ridge, Tennessee, Oak Ridge Gaseous Diffusion Plant, Union Carbide Corporation, Nuclear Division (November, 1967).

24. Wakao, N., and Smith, J. M., "Diffusion in Catalyst Pellets," Chem. Engr. Sci. *17*, 825-834 (1962).

25. Wakao, N., and Smith, J. M., "Diffusion and Reaction in Porous Catalysts," I. & E. C. Fund. *3*, 123-127 (1964).

26. Whatley, M. E., "Unit Operations Section Monthly Progress Report, August-September, 1964," ORNL-TM-1027, Oak Ridge, Tennessee, Oak Ridge National Laboratory, Union Carbide Corporation, Nuclear Division (March, 1965).

27. Wheeler, A., "Reaction Rates and Selectivity in Catalyst Pores." Catalysis, Vol. II., pp. 105-165, Reinhold Publishing Corporation, New York (1955).

28. Young, D. M., and Crowell, A. D., "Physical Adsorption of Gases," pp. 1-3, Butterworth, Inc., Washington (1962).

APPENDIXES

APPENDIX A

FORTRAN PROGRAM FOR SOLUTION OF THE MODEL EQUATIONS

The digital computer program shown in Table I effects the solution of the model equations describing the adsorption of uranium hexafluoride on fixed beds of sodium fluoride. Use of the program requires specification of the following information:

1. Pellet surface area, sq m/g,
2. Breakthrough concentrations, lb of UF_6/lb of inert,
3. Bulk density of sorbent bed, lb/cu ft,
4. Time increment size, hr,
5. Bed increment size, ft,
6. Density of sorbent pellet, lb/cu ft,
7. Density of diluent gas at 32°F and 1 atm, lb/cu ft,
8. Bulk diffusivity of reacting component in diluent gas at temperature and pressure of system, sq ft/hr,
9. Void fraction of pellets,
10. Mole fraction of reacting component in gaseous feed,
11. Mass flow rate of diluent gas, lb/sq ft-hr,
12. Maximum loading of uranium hexafluoride on sodium fluoride pellet, lb of UF_6/lb of NaF,
13. Time interval between print outs, hr,
14. Total pressure of system, atm,
15. Temperature of system, °R,

TABLE I

PROGRAM

```
C  DYNAMIC ADSØRPTIØN ØF URANIUM HEXAFLUØRIDE
       DIMENSIØN QTØT(400),Q(400),D(400),PSEUDØ(400),CB(400)
     2 READ(5,200)LAST
       READ(5,201)APELLT,BREAK,BUKDEN,DELTME,DELZ,DENSØR,
      .DENSTY,DIFF,EPSIØ,FRACT,GN,QMAX,PTIME,PTØT,TEMP,TEST,
      .TRAPA,WTPEL
   200 FØRMAT(I5)
   201 FØRMAT(5F10.0)
C QUANTITIES CHARACTERISTIC ØF UF6-N2-NAF SYSTEM
       BMØLWT=28.0
       CMØLWT=352.0
       C1=32.60
       C2=31470.0/(QMAX*(1.0-EPSIØ))
       C3=3816.0
       TEMPK=TEMP/1.8
       UF6MU=0.0001491*TEMPK**0.933
       AN2MU=0.00348*TEMPK**1.5/(TEMPK+118.0)
       AMU=UF6MU*FRACT+AN2MU*(1.0-FRACT)
C QUANTITIES CHARACTERISTIC ØF HARSHAW PELLETS
       ASPHRE=0.00150
       RN=0.00624
       C4=2.0
C SET INITIAL VALUES
       AMØLWT=FRACT*CMØLWT+(1.0-FRACT)*BMØLWT
       AMWNEW=AMØLWT
       G=AMØLWT*GN/((1.0-FRACT)*BMØLWT)
       GNEW=G
       CBIN=(G-GN)/GN
       CB(1)=CBIN
       BPØRØ=1.0-BUKDEN/DENSØR
       DENSTY=DENSTY*491.7/TEMP*PTØT*(1.0-FRACT)
       APELLT=APELLT*10000.0
       SUMQ=0.0
       H1=DIFF*EPSIØ*C4
       H2=C1*DENSØR*APELLT*EXP(-C3/TEMP)
       H3=(-C2/APELLT)
       H5=0.730*TEMP/CMØLWT
       UF6FLØ=GN*TRAPA*CBIN
C ØUTPUT PHYSICAL PRØPERITIES ØF SYSTEM FØR IDENTIFICATIØN
       WRITE(6,203)
```

TABLE I (Continued)

```
203 FØRMAT(1H1,
    •44HURANIUM HEXAFLUØRIDE ADSØRPTIØN CALCULATIØNS)
     WRITE(6,204)APELLT,EPSIØ,DENSØR,WTPEL,RN,ASPHRE,QMAX,
    •BUKDEN,TRAPA,DELZ,TEMP,LAST
     WRITE(6,206)G,GN,CBIN,BREAK,FRACT,PTØT,AMØLWT,BMØLWT,
    •DENSTY,DIFF,AMU,TEST,DELTME
     WRITE(6,205)C1,C2,C3,C4
204 FØRMAT(1HO,22HSURFACE AREA SQ CM/GM ,F10.2,3X,
    •16HPELLET PØRØSITY ,F8.5/1H ,
    •24HPELLET DENSITY LB/CU FT ,F9.5,2X,
    •17HPELLET WEIGHT LB ,F10.8/1H ,17HPELLET RADIUS FT ,
    •F10.8,8X,29HEFFECTIVE TRANSFER AREA SQ FT ,F10.8/1H ,
    •21HPELLET LØADING LB/LB ,F10.5,4X,
    •22HBULK DENSITY LB/CU FT ,F10.2/1H ,
    •25HTRAP CRØSS SECTIØN SQ FT ,F8.5,2X,
    •22HINCREMENTAL HEIGHT FT ,F8.4/1H ,
    •24HTRAP TEMPERATURE RANKINE,F6.1,5X,
    •26HNUMBER ØF BED INCREMENTS =,I4/1HO)
205 FØRMAT(1H ,4HC1 =,E15.5,5X,4HC2 =,E15.5/1H ,5HE/R =,
    •E15.5,5X,7H1/TAU =,E15.5/1HO)
206 FØRMAT(1HO,22HMASS FLØW LB/HR SQ FT ,F10.4,3X,
    •23HINERT FLØW LB/HRSQ FT ,F10.4/1H ,
    •25HINLET CØNCENTRATIØN LB/LB,F8.5,2X,
    •18HBREAK PØINT LB/LB ,F8.5/1H ,
    •20HINLET MØLE FRACTIØN ,F8.7,7X,
    •19HTØTAL PRESSURE ATM ,F6.3/1H ,
    •21HAVG MØLECULAR WEIGHT ,F10.5,4X,
    •23HINERT MØLECULAR WEIGHT ,F10.5/1H ,
    •23HINERT DENSITY LB/CU FT ,F10.8,2X,
    •20HDIFFUSIVITY SQ FT/HR,F10.8/1H ,
    •19HVISCØSITY LB/FT HR ,F10.8,6X,17HLENGTH ØF RUN HR ,
    •F6.2/1H ,18HTIME INCREMENT HR ,F6.4/1HO)
     TIME=0.0
     PRNT=PTIME*0.99995
 30  DØ 90 INCRE=1,LAST
     IF(TIME)32,32,43
 32  QTØT(INCRE)=0.0
 36  Q(INCRE)=0.0
     D(INCRE)=H1
 38  PSEUDØ(INCRE)=H2
 43  IF(CB(INCRE))44,44,46
 44  CB(INCRE+1)=0.0
     GØ TØ 90
 46  IF(D(INCRE))76,76,48
```

TABLE I (Continued)

```
   48 SRBID=SQRT(PSEUDØ(INCRE)/D(INCRE))
   50 PHI=12.571*RN*D(INCRE)*(SRBID*RN/TANH(SRBID*RN)-1.0)
      ANRE=2.0*RN*G/AMU
      ANSC=AMU/(DIFF*DENSTY)
      AJMASS=(1.0/BPØRØ)*(0.010+0.863/((ANRE)**0.58-0.483))
      PB=CB(INCRE)*AMØLWT*PTØT/((1.0+CB(INCRE))*CMØLWT)
      PGF=PTØT-0.333*PB
      DØ 55 I=1,4
      AKGA=AJMASS*G/(PGF*(ANSC)**0.6667)*ASPHRE
      CS=PB*AKGA/(PHI+H5*AKGA)
      PSN=CS*H5
      PBI=PTØT-PB
      PSNI=PTØT-PSN
   55 PGF=(PSNI-PBI)/ALØG(PSNI/PBI)
   60 TRATE=CS*PHI
C    TØTAL RATE EQUALS PØUND PER PELLET
      RATE=TRATE/WTPEL
C RATE EQUALS PØUND PER PØUND
      QØLD=Q(INCRE)
      QCØR=QMAX-QØLD
      Q(INCRE)=QMAX-QCØR*EXP(-RATE*DELTME/QCØR)
      D(INCRE)=H1*(1.0-Q(INCRE)/QMAX)
      IF(D(INCRE))75,75,81
   75 D(INCRE)=0.0
      Q(INCRE)=QMAX
      EZ=QTØT(INCRE)
      QTØT(INCRE)=Q(INCRE)*BUKDEN*TRAPA*DELZ
      SUMQ=SUMQ+QTØT(INCRE)-EZ
      PSEUDØ(INCRE)=H2*EXP(H3*QMAX)
   76 CB(INCRE+1)=CB(INCRE)
      GØ TØ 90
   81 PSEUDØ(INCRE)=H2*EXP(H3*Q(INCRE))
C    CALCULATIØN ØF CØNCENTRATIØN LEAVING INCREMENT
C              USING RUNGE-KUTTA
   82 QUAN=BUKDEN*PHI*AMØLWT*PTØT*AKGA/((GN*WTPEL)*(CMØLWT*
     .PHI+0.730*AKGA*TEMP))
      Z1=(-QUAN)*CB(INCRE)/(1.0+CB(INCRE))*DELZ
      Z2=(-QUAN)*(CB(INCRE)+Z1/2.0)/(1.0+CB(INCRE)+Z1/2.0)*
     .DELZ
      Z3=(-QUAN)*(CB(INCRE)+Z2/2.0)/(1.0+CB(INCRE)+Z2/2.0)*
     .DELZ
      Z4=(-QUAN)*(CB(INCRE)+Z3)/(1.0+CB(INCRE)+Z3)*DELZ
      CB(INCRE+1)=CB(INCRE)+0.16667*(Z1+2.0*Z2+2.0*Z3+Z4)
      AJØBDØ=G-GN
```

TABLE I (Continued)

```
      IF(CB(INCRE+1))83,84,84
   83 CB(INCRE+1)=0.0
   84 G=G-RATE*BUKDEN*DELZ
      IF(GN-G)86,85,85
   85 G=GN
      UF6FL0=0.0
      CB(INCRE+1)=0.0
      ITRACK=INCRE
      Q(INCRE)=Q0LD + AJ0BD0*DELTME/(BUKDEN*DELZ)
      PSEUD0(INCRE)=H2*EXP(H3*Q(INCRE))
      QT0T(INCRE)=QT0T(INCRE)+AJ0BD0*DELTME*TRAPA
      SUMQ=SUMQ+AJ0BD0*DELTME*TRAPA
      AJ0BD0=0.0
      G0 T0 87
   86 UF6FL0=UF6FL0-RATE*BUKDEN*TRAPA*DELZ
      EZ=QT0T(INCRE)
      QT0T(INCRE)=Q(INCRE)*BUKDEN*TRAPA*DELZ
      SUMQ=SUMQ+QT0T(INCRE)-EZ
   87 AM0LWT=(GN*TRAPA+UF6FL0)/(GN*TRAPA/BM0LWT+UF6FL0/
     .CM0LWT)
   90 C0NTINUE
C    C0NTR0L RETURNS T0 STATEMENT N0 30
      TIME=TIME+DELTME
      G=GNEW
      UF6FL0=GN*TRAPA*CBIN
      AM0LWT=AMWNEW
   92 IF(CB(LAST).GE.BREAK)G0 T0 120
   94 IF(TIME.GE.TEST)G0 T0 122
   96 IF(TIME.LE.PRNT)G0 T0 30
      PRNT=PRNT+PTIME
      WRITE(6,210)TIME,CB(LAST),SUMQ,ITRACK
  210 F0RMAT(1H0,15HTIME IN H0URS =,F6.2/1H ,
     .15HC0NCENTRATI0N =,E15.5,5X,14HT0TAL H0LDUP =,E15.5,
     .5X,7HTRACK =,I4)
   98 G0 T0 30
  120 WRITE(6,214)TIME,CB(LAST),SUMQ
      G0 T0 2
  122 WRITE(6,220)TIME,CB(LAST),SUMQ
      G0 T0 2
  214 F0RMAT(1H0,18HBREAKTHR0UGH AFTER,F6.2,1X, 5HH0URS/1H ,
     .28HBREAKTHR0UGH C0NCENTRATI0N =,E15.5/1H ,
     .20HS0RBENT BED H0LDUP =,E15.5)
```

TABLE I (Continued)

```
220 FØRMAT(1HO,32HBREAKTHRØUGH DID NØT ØCCUR AFTER,F6.2,
    •2X,5HHØURS/1H ,21HFINAL CØNCENTRATIØN =,E15.5/1H ,
    •20HSØRBENT BED HØLDUP =,E15.5)
     END
```

16. Length of run, hr,

17. Trap cross sectional area, sq ft, and

18. Average weight of single pellet, lb.

The program is divided into appropriately labeled sections which are, for the most part, straightforward. An attempt has been made to use nomenclature in the program that follows very closely that used in the text of this thesis.

APPENDIX B

DIFFUSION COEFFICIENTS IN BINARY GAS SYSTEMS

Reid and Sherwood [20] recommend that the bulk diffusion coefficient D_{12} for a binary gas mixture at pressures less than 15 atm be estimated by

$$D_{12} = \frac{0.001858\ T^{3/2}\ [(M_1 + M_2)/M_1M_2]^{1/2}}{P\sigma_{12}^2\ \Omega_D}$$

where D_{12} = diffusion coefficient for binary system, sq cm/sec,

T = temperature, °K,

M_1, M_2 = molecular weights of components 1 and 2,

P = total pressure, atm,

$\sigma_{12} = \frac{1}{2}(\sigma_1 + \sigma_2)$, σ_1 and σ_2 are Lennard-Jones force constants for components 1 and 2, Å, and

Ω_D = collision integral from available tabulations [20].

The force constants for uranium hexafluoride, as given by DeMarcus and Starnes [8] are:

$$\sigma = 5.2232\ \text{Å}, \text{ and}$$

$$\varepsilon/k = 439°\text{K}.$$

For nitrogen, Reid and Sherwood [20] give the values:

$$\sigma = 3.681\ \text{Å}, \text{ and}$$

$$\varepsilon/k = 91.5°\text{K}.$$

These values were used to determine the diffusivity of uranium hexafluoride in nitrogen at 1 atm as shown in Table II.

TABLE II

DIFFUSIVITY OF URANIUM HEXAFLUORIDE IN NITROGEN
AT ATMOSPHERIC PRESSURE

Temperature, °F	D_{12}, sq ft/hr	Temperature, °F	D_{12}, sq ft/hr
40	0.265	180	0.423
60	0.286	200	0.449
80	0.308	220	0.478
100	0.335	240	0.504
120	0.353	260	0.531
140	0.376	280	0.558
160	0.400	300	0.585

APPENDIX C

VISCOSITY OF BINARY GAS MIXTURES

To estimate the viscosity of a binary mixture of gases at low pressure, Reid and Sherwood [20] recommend:

$$\mu_{mix} = \frac{\mu_1}{1 + (y_2/y_1)\phi_{12}} + \frac{\mu_1}{1 + (y_1/y_2)\phi_{21}}$$

where μ_{mix} = viscosity of mixture,

μ_1, μ_2 = viscosity of pure components,

y_1, y_2 = mole fraction of component 1 and 2,

$$\phi_{12} = [1 + (\mu_1/\mu_2)^{1/2}(M_2/M_1)^{1/4}]^2/[2\sqrt{2}\ (1 + M_1/M_2)^{1/2}],$$

$$\phi_{21} = [1 + (\mu_2/\mu_1)^{1/2}(M_1/M_2)^{1/4}]^2/[2\sqrt{2}\ (1 + M_2/M_1)^{1/2}].$$

The viscosity of gaseous uranium hexafluoride, reported by DeWitt [9], is expressed as:

$$\mu = 0.6163\ T^{0.933}$$

where T is the temperature in degrees Kelvin, and μ is expressed in micropoise. The correlation was obtained from experimental data taken between 40 and 200°C.

The viscosity of nitrogen is given [19] in the temperature range of 15 to 100°C as

$$\mu = 0.00144\ \frac{T^{3/2}}{T + 118},$$

where T is the temperature in degrees Kelvin and μ is expressed in centipoise.

For the uranium hexafluoride-nitrogen system, within a reported temperature range of 29 to 100°C and uranium concentration of 0.57 to 8.7 mole percent, McNeese [17] found that the viscosity could be represented to within less than one percent of values calculated from the recommended equation by the ideal relation

$$\mu_{mix} = \mu_1 y_1 + \mu_2 (1 - y_1) .$$

The ideal relation was used in this work to calculate the viscosity of the uranium hexafluoride-nitrogen mixture.

APPENDIX D

ACCURACY OF THE NUMERICAL SOLUTION

Numerical methods are often used by the engineer to solve problems which are otherwise too complicated for analytical solutions. The accuracy of the analysis, of course, depends upon the number of increments employed to effect the solution. Increase in accuracy is generally at the expense of increased computer time. An estimate of the degree of convergence or accuracy of the final result can ordinarily be obtained by comparing calculations made using incremental steps of varying size [18].

The operating parameters of the fourth run presented in Chapter V were arbitrarily selected as typical for purposes of demonstrating the convergence characteristics of the mathematical model. For this run, a total gas flow rate of 5.56 lb mole/sq ft-hr and gas concentrations of 2.80 mole percent uranium hexafluoride were maintained. The sorbent trap was charged to a height of 4 feet with 24.4 pounds of sodium fluoride and was operated at a temperature of 250°F. A family of curves representing the total bed loading after one hour of operation for time increments up to 0.10 hour and bed increments from 0.02 to 0.07 feet was generated and is presented in Figure 18. The curves tend to converge to 4.84 pounds of uranium hexafluoride, a value which is identical to the bed loading calculated from an overall material balance. Conveniently, the material balance check can be used to estimate the degree of

DWG. NO. G-68-1004

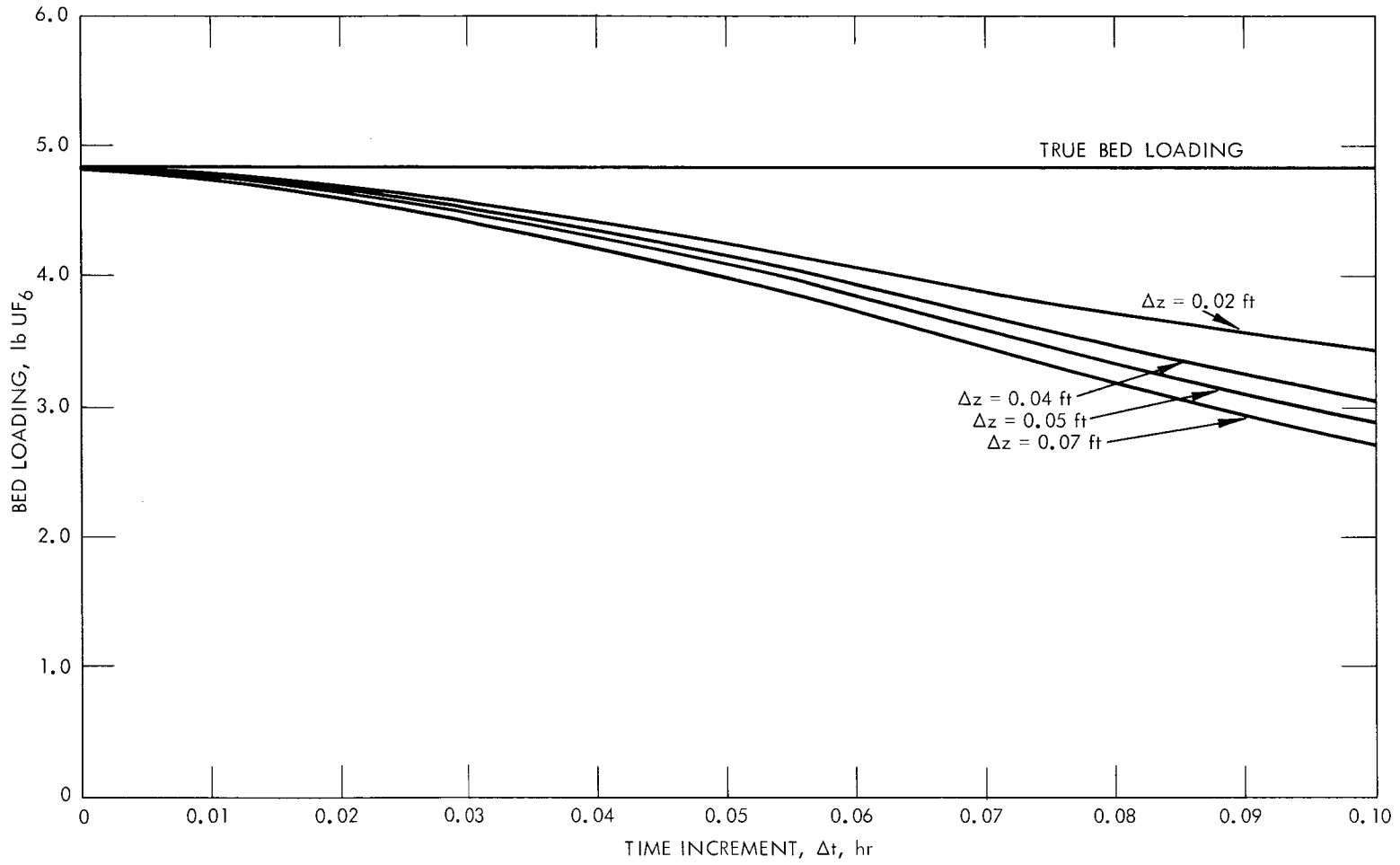

FIGURE 18

CONVERGENCE BEHAVIOR OF NUMERICAL SOLUTION FOR TYPICAL RUN

convergence for each run. The comparison, of course, is not meaningful after breakthrough.

For the test case, the model solution appeared to become unstable with bed increments larger than around 0.09 foot, producing curves which varied irregularly from the general shape of those calculated for smaller bed increments. On the other hand, runs with bed increments smaller than 0.02 foot were found to require amounts of computer time considered excessive relative to the increase in accuracy obtained. All calculations for this work were performed using time increments of 0.01 hour and bed increments of 0.05 foot. In general, the calculated bed loadings were found to be within 97 to 98 percent of their true values.

APPENDIX E

ESTIMATION OF MAXIMUM PELLET LOADING

The general results of the study by McNeese [17,26] are presented in Figures 19 and 20. From these results, the maximum loading of uranium hexafluoride on pelleted sodium fluoride can be estimated. For more exact results, if experimental data are not available, the complete work should be consulted.

Figure 19 shows the dependence of pellet loading upon the adsorption temperature and pellet surface area. The results are based on an operating pressure of 1 atm. The pellets were assumed to be in the form of standard 1/8-inch right circular cylinders as manufactured by the Harshaw Chemical Company and to have a void fraction of 0.45.

Figure 20 shows the dependence of pellet loading upon the adsorption temperature and pellet void fraction. Again, an operating pressure of 1 atm and standard Harshaw pellets are assumed. The calculations are based upon pellets having a surface area of 0.85 sq m/g.

DWG. NO. G-68-1005

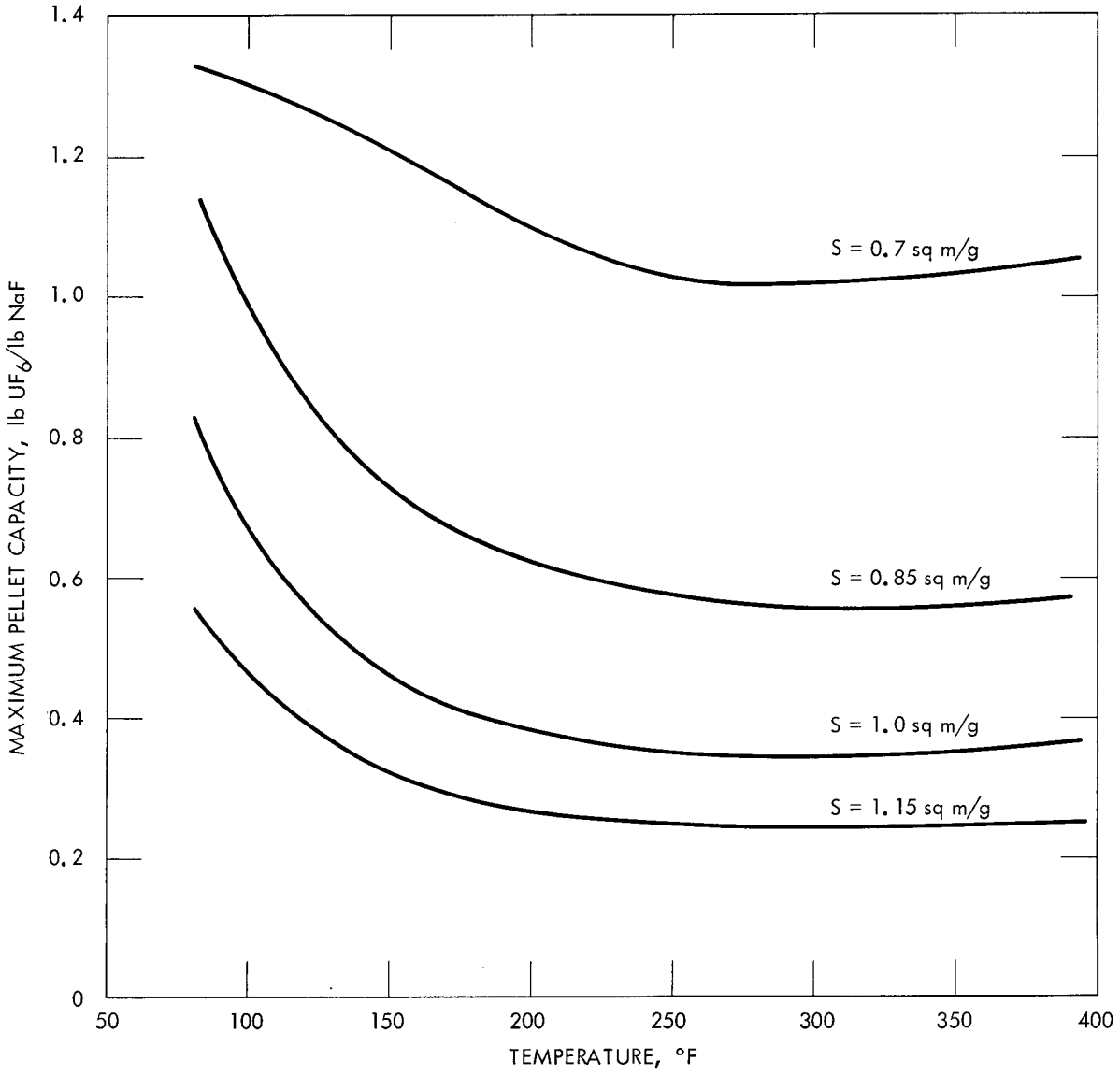

FIGURE 19

PREDICTED MAXIMUM PELLET LOADING AS A FUNCTION OF TEMPERATURE AND PELLET SURFACE AREA

DWG. NO. G-68-1006

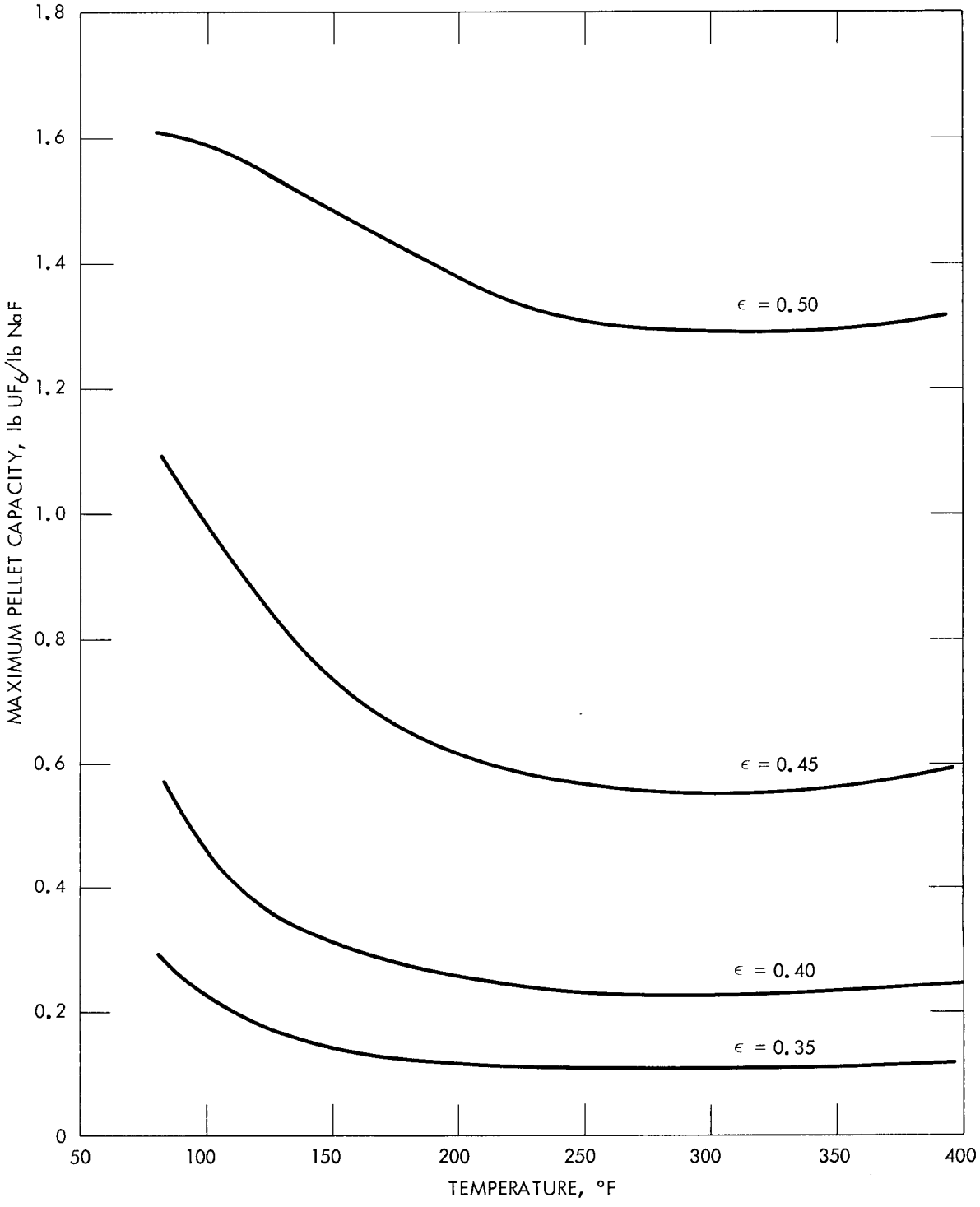

FIGURE 20

PREDICTED MAXIMUM PELLET LOADING AS A FUNCTION OF TEMPERATURE AND PELLET VOID FRACTION

LIST OF SYMBOLS

a	Effective mass transfer area, sq ft/pellet,
C_A	Concentration of adsorbing component within the pellet, lb of A/cu ft,
C_{Ab}	Concentration of component A in the bulk gas stream, lb of A/lb of inert,
C_{As}	Concentration of adsorbing component on the surface of the pellet, lb of A/cu ft,
C_1	Constant of reaction rate equation, cu ft/lb-hr-(area/mass),
C_2	Constant of reaction rate equation, area/mass,
D_{AB}	Bulk diffusivity of component A in B, sq ft/hr,
D_{eff}	Effective diffusivity of component A in porous media, sq ft/hr,
$\overline{D}_{eff}$	Average effective diffusivity of component A in pellet, sq ft/hr,
D_K	Knudsen diffusivity, sq ft/hr,
D_p	Effective pellet diameter, ft,
E	Activation energy for diffusion, Btu/lb-mole,
G	Mass flow rate of gas mixture, lb/hr-sq ft,
G_N	Mass flow rate of inert gas, lb/hr-sq ft,
jd	Mass transfer factor, dimensionless,
K_g	Molar mass transfer coefficient, lb-mole/hr-sq ft-atm,
k_1'	Pseudo first order reaction rate constant, 1/hr,
$\overline{k_1'}$	Average pseudo first order reaction rate constant for entire pellet, 1/hr,
M_m	Mean molecular weight, lb/lb-mole,

N_A Molar flux of component A, lb-mole/hr-sq ft,

N_{Re} Reynolds number, D_pG/μ, dimensionless,

$N_{Re'}$ Modified Reynolds number, $D_pG/\mu(1-\varepsilon_B)$, dimensionless,

p_{gf} Log-mean partial pressure of inert component in "film", atm,

P Pressure, atm,

q_A Loading of component A on sorbent, lb of A/lb of sorbent,

q_{max} Maximum point loading of component A on sorbent, lb of A/cu ft,

$\overline{q}_{max}$ Maximum average loading of component A on sorbent, lb of A/lb of sorbent,

q_r Amount of uranium hexafluoride complexed at a given point r within the pellet, lb/cu ft,

R Ideal gas constant, Btu/lb-mole-°R,

R Radius of pellet, ft,

r_A Total rate of reaction of component A with pellet, lb of A/lb of sorbent-hr,

r_p Pore radius, ft,

S Surface area of pellet, area/mass,

T Temperature, °R,

t Time, hr,

W_A Mass flow of adsorbing component A to pellet, lb/hr-pellet,

w Average weight of sorbent pellet, lb,

z Axial distance of penetration into the bed, ft,

ε Porosity of pellet, void volume/total volume, dimensionless,

μ Viscosity of gas mixture, lb/ft-hr,

ρ Density of gas mixture, lb/cu ft,

ρ_B Bulk density of sorbent bed, lb/cu ft,

ρ_{NaF} Density of sodium fluoride pellet, lb/cu ft,

τ Tortuosity factor, dimensionless.

VITA

The author was born July 24, 1943, in Charleston, West Virginia. He attended grammar school at Oak Ridge, Tennessee, and was graduated from Oak Ridge High School in 1961. He enrolled at the University of Tennessee and was graduated with honors in 1965 with a B.S. in Chemical Engineering.

In 1965, the author was employed by the Technical Division of the Oak Ridge Gaseous Diffusion Plant and began graduate study the following year in the evenings with the Oak Ridge Resident Graduate Program.

The author married the former Miss Ellen Sue Jones in 1967, and they have no children, save two parakeets and a very friendly brown-haired dog.

The author is an associate member of the American Institute of Chemical Engineers and a member of Tau Beta Pi and Phi Kappa Phi.